Physically Stimulated Nanotheranostics for Next Generation Cancer Therapy: Focus on Magnetic and Light Stimulation

Nanasaheb D. Thorat[1,2], Syed A. M. Tofail[2], Brigitte von Rechenberg[3], Helen Townley[4] Hemraj M. Yadav[5], Thomas Steffen[3] and Joanna Bauer[1].

[1] Department of Biomedical Engineering Wroclaw University of Science and Technology Wroclaw, Poland.

[2] Department of Physics, Bernal Institute, University of Limerick, Limerick, Ireland.

[3] Musculoskeletal Research Unit (MSRU), Competence Center for Applied Biotechnology (CABMM) Vetsuisse Faculty ZH, University of Zurich, Zurich, Switzerland.

[4]Nuffield Department of Women's & Reproductive Health, University of Oxford, Oxford, UK.

[4] Department of Materials and Engineering, Dongguk University, Seoul, South Korea

Abstract:

Physically or externally stimulated nanostructures often employ multimodality and show encouraging results at pre-clinical stage in cancer therapy. Specially designed smart nanostructures such as hybrid nanostructures are responsive to external physical stimuli such as light, magnetic field, electric, ultrasound, radiofrequency, X-ray, etc. These physically responsive nanostructures have been widely explored as non-conventional innovative 'nanotheranostics' in cancer therapies. Physically stimulated (particularly magnetic and light) nanotheranostics provide a unique combination of important properties to address key challenges in modern cancer therapy: (i) an active tumour targeting mechanism of therapeutic drugs driven by a physical force rather than passive antibody matching, (ii) externally/remotely controlled drugs on demand release mechanism, and (iii) a capability for advanced image guided tumour therapy and therapy monitoring. Although primarily addressed to the scientific community, this review offers valuable and accessible information for a wide range of readers interested in the current technological progress with direct relevance to the physics, chemistry, biomedical field and theranostics. We herein cover magnetic and light triggered modalities currently being developed for non-conventional cancer treatments. The physical basis of each modality is explained so readers from physics, materials science background can grasp new developments in this field easily.

I. Introduction
II. Concept of physically stimulated nanotheranostics
III. Magnetic-Stimulated Nanotheranostics
    A. Magnetically guided drug delivery
        a. Underlying physics
        b. Clinical progress
    B. Magnetic fluid hyperthermia
        a. Underlying physics
        b. Clinical progress
    C. Magnetic imaging
        a. Underlying physics
            1. Magnetic Resonance Imaging
            2. Magnetic Particle Imaging
        b. Clinical progress
    D. Future opportunities and challenges
IV. Light-Stimulated Nanotheranostics
    B. Photodynamic therapy
        a. Underlying physics
        b. Clinical progress
        c. Next generation PDT device design
    C. Photothermal therapy
        a. Underlying physics
        b. Classification of nano PTAs
        c. Clinical progress
        d. Next generation device design
    D. Two-Photon light therapy
        a. Underlying physics
        b. Clinical progress
    D. Future opportunities and challenges
V. Conclusion: The promise of physically stimulated cancer nanotheranostics

I. Introduction:

Current cancer therapies usually lack the focus to provide specific therapeutic drug delivery to only the tumour, and it is remains one of the greatest challenges in cancer therapy. Chemotherapy and radiotherapy are the main pillars of conventional cancer therapies for almost all type of cancers. However, advancement in both therapies could not result in patient survival rate beyond 30 %.[1] These therapies also have several limitations such as severe toxic side effects on patients health for example damage to immune systems.[2,3] Continuous doses of chemotherapeutic drugs to a tumour induce drug resistance (chemoresistance) mechanisms in cancer cells, and this ultimately results in the failure of chemotherapy. Development of next generation cancer therapies has thus been a vital need for better outcome of patient's health. Among many non-conventional cancer therapeutic strategies being interrogated in the last decade, therapies that are responsive to external physical stimuli are of particular interest can have advantage over conventional therapies. Many research groups have published novel ways to utilize nanoscale agents that are capable of responding to physical stimulus such as (i) light (ii) magnetic field (iii) ultrasound (iv) radiofrequency, and (v) X-ray. Specially designed nanostructures termed hybrid nanostructures (HNCs) are highly sensitive to physical stimulus and can perform 'on demand' cancer theranostics (therapy + diagnostics).[4] The term "theranostics" symbolizes a new class of treatment options that are capable of providing both therapy and diagnostics to patients[5].

Taking advantage of the interesting physical properties of different nanomaterials especially HNCs, a variety of different physical stimuli theranostics strategies have been exploited as next generation cancer therapeutics.[6] Unlike conventional cancer therapies, such as chemotherapy and radiotherapy usually lead with side effects. Nowadays, the term 'nanotheranostics' implies an inclusive set of physical principles, engineer means nanotechnological and biochemical approaches, offering various prospects for therapy and diagnostics. Physically stimulated nanotheranostics could destroy cancer tissues/tumours only under specific external stimuli, and thus could offer fewer side effectswith enhanced treatment specificity. Additionally, physically responsive nanomedicine can also be combined with other conventional cancer treatments, such as chemotherapy, to achieve synergistic anticancer effects *via* a different diverse biochemical and physical mechanisms. Use of externally applied physical stimuli such as magnetic or light signals in the form of physical forces along with administered signalling molecules i.e. HNCs could allow for chemotherapeutic drug presentation at the right time and at the right dose, this is the main requisite of cancer therapy.

Nanotheranostics usually refers to integrating imaging and therapy functions of nanoscale materials or nano-agents within a single modality.[7] On the other hand 'theranostic' which refers to concurrenttherapy and diagnosis of disease has been a popular concept in recent years, especially in the cancer field. Researchers and oncologists believe integration of diagnosis and therapy in a single modality would offer real advantages over independently conducted diagnosis and therapy.[8] The physically stimulated (light/magnetic) nanotheranostics initiates a cascade of events in tumours due to the external physical force (magnetic) or trigger (light), which in turn could be employed for diagnostic imaging, therapy, or both simultaneously.[9] This unique approach, offering superior spatiotemporal control of acquisition features and nanoprobe monitor of the disease. Most of the HNCs are being used as intrinsic stimuli-responsive system whether they react to endogenous or exogenous *in vivo* stimuli such as pH,[10] enzymes,[11,12] redox,[13,14] hypoxia,[15,16] of the cell/tumor microenvironment. These *in vivo* stimuli are restricted to inside body/organism system, with the tumor microenvironment and the use of stimuli can result in an uncontrolled release of the chemotherapeutic payload. It is anticipated that these drawbacks could potentially be overcome by using HNCs in combination with magnetic and light activated remote triggering.

Though numerous examples of physically stimulated HNCs nanotheranostics based cancer therapeutic interventions exist, our motivation and rationale for suggesting this review was to argue that with the rapid development of magnetic and light stimulated nanotheranostics for next generation cancer therapy applications *then what?? – unfinished sentence*. Recent progress in developing newer smart nanostructures has indeed shed new light and prospects on non-conventional cancer theranostics due to unique physicochemical properties of these nanostructures. While the potential of intrinsic or biochemical stimuli-responsive nanotheranostics to capitalize delivery properties of chemotherapeutics for cancer treatment is widely documented[17–21] in contrast, magnetic and light stimulated nanotheranostics and their biomedical applications in cancer therapy remain relatively contemporary. Concerning cancer, nanotheranostics approaches have been developed in the laboratories, with some technologies successfully translated into the clinical stage. Without being exhaustive, the objective of this original review was to focus physics of the nanotheranostics response to magnetic and light stimulation. The term 'physical stimuli' in this review deals with magnetic field and light.

The approach of physical stimulation/triggering is, however, more diverse and is not limited to magnetic and light triggering only. As mentioned above physical stimulation/triggering encompass by a variety of stimuli such as ultrasound, electrical field, electromagnetic field and magneto-electric triggering. The advantage of each triggering modality in the broad field of

cancer nanomedicine over conventional cancer treatments has been reviewed, recently[22]. Among all these noninvasive and controlled modalities, magnetic and light stimulation are highly sensitive to external and internal environments and advancing clinical practices, in recent decades. Fortunately, magnetic and light triggers have fewer side effects, are easily accessible, and can be smoothly manipulated for excellent controllability, making them favourable for cancer theranostics. Thus, the current review is focused on these two physical stimulation modalities to promote remarkable advancement of magnetic and light stimulated cancer nanotheranostics to material scientists, clinicians, oncologists, radiologists, and patients. The smart materials or HNCs reviewed here can integrate 'controlled' cancer theranostics into a solitary platform, which is a revolutionary advancement in the path towards highly safe and effective personalized cancer therapy[23]. We conclude by providing an outlook on current challenges and opportunities, and explore potential research directions towards accelerating the development and translation of the physically stimulated nanotheranostics for next generation cancer therapy.

II. Concept of physically stimulated nanotheranostics

For millions of years, mammals have been improving their immature and unstable brain activities by physical stimulation. The established ideal example of such physical stimulation is the mother and baby; brain activity of the baby can only increase and stabilize after frequent stimulation by means of physical contact with mother. This external physical or mechanical triggering can quickly stimulate neurons electrically and increase the response in the brain of young children. Excitingly, in the last few years a range of physical stimulation strategies have emerged to treat various human diseases; primarily cancer[4,24] and Alzheimer's.[25,26] Among these and other diseases, physical stimulation has attained moderate advantages for cancer theranostics in combination with nanomedicine. Achieving adequate cancer cell targeting and killing with high specificity while sparing normal cells, physical stimulation is relying on nanomedicine.. In recent years, nanomedicine combined with radiofrequency, X-ray and electric field are also proposed as novel physical stimulation strategies.

Although significant progress has been attained on internal ''triggers'' such as temperature, pH, redox potential and enzymes. Such a pathological or *in vivo* stimulation can be executed in a static passive mode and faces challenges of chemotherapeutic dosage control, timing and duration of the therapeutic drug release. Moreover, the *in vivo* stimulation approach would not allow for self-regulated controlled chemotherapeutic cargo release. In the treatment of cancer, prior drug release kinetics and drug dosing is difficult to predict. To achieve high

therapeutic potential, drug dosing will need to be actively managed. This could benefit from regulated drug performance made possible through extraneous control over drug release. The use of externally applied signals in the form of physical forces along with administered signaling nanostructures could allow for drug release at the right time and at the right dose needed for a cancer patient[27].

As of today, a broad variety of physical stimulation systems are engineered and described that are proficient as remotely controlled theranostics modalities. These systems underlying basic physics principles and responding to more than one stimulus simultaneously in both intrinsic and external mode. Physical stimulation strategies coupled with smart hybrid nanostructures facilitate a desirable way for incorporated drug molecule activation.Their on-demand release can be achieved by local internalization of nanostructures which have high penetration into cells [19]. Biophysical energy such as magnetic fields, ultrasound, electric fields and mechanical forces, light and temperature gradients can act as enhancers for nanotheranostics[28]. Each form of physical energy has been associated with a novel technique in cancer or nanotheranostics. Examples include magnetic fields for magnetoporation[29] and magnetic field drug targeting[30], electric current/potential for electroporation[31] and iontophoresis[32], ultrasound for sonodynamic therapy[33] and sonoporation[34], pulsed light for optoporation and drug release[35], and temperature for thermoporation and hyperthermia therapy[36]. This review is motivated by the rapidly increasing field of cancer nanotheranostics and the number of publications investigating the potential of novel physically stimulated strategies (i) to enhance remotely controlled and triggered drug delivery to tumor, (ii) to induce hyperthermia ablation using different types of magnetic nanoparticles (MNPs), or near infrared (NIR) light induced hyperthermia using gold nanorods, (iii) to enhance radiotherapy in a clinical setting and with hybrid nanostructures as theranostic agents particularly magnetic@gold, silica@silver, carbon@gold or gadolinium, (iii) to promote a photodynamic effect with multifunctional hybrid nanostructures, and (iv) to permeate the blood-brain barrier (BBB) using MNPs.

As far as physical stimulus or responsive therapies are concerned, nanotheranostics however, may have its unique advantage. Unlike chemotherapy which applies to the whole body, external physical stimulus-responsive nanotheranostics are often applied locally onto the tumour[4]. Real-time monitoring of chemotherapeutic agents distributed in the whole body, particularly in the tumour is essential for maximal therapeutic outcome. Existent conventional chemotherapeutics modalities have limited monitoring window during and after the treatment. On the other hand, physically stimulated nanotheranostics, e.g. ight, magnetic field, ultrasound, , allows a real monitoring window of the distribution of therapeutic agents. Thus, physically

stimulated nanotheranostics applied at the best timing is opening effective therapeutic options by combining imaging required to real-time monitor of tumor when the stimulus-responding nanostructures reaches its maximal level in the tumor after its administration. In addition, nanotheranostics coupled with imaging modalities could also be helpful to monitor the under or over dosed therapeutic responses (e.g. optical energy, X-ray dose, etc.) under physical stimuli.

III. Magnetic-Stimulated Nanotheranostics

Every living organism on the planet is under continuous exposure of the Earth's natural magnetic field (MF). This magnetic field consists of two components, the first one is a gradually changing quasi-static component with flux density (BE) ≈ 30–60 μT, the other component (BS) has a magnitude 2 or 3 orders less than that of BE and consists of dynamic fluctuations with a wide range of frequencies from a few Hz to several kHz[37]. During the twentieth century industrial revolution, numerous man-made technogenic electromagnetic field (EMF) sources were added to the natural ones. These man-made systems such as power lines, electrotechnological industrial machines, telecommunication facilities, consumer electronics, medical equipment, and many others produce high magnetic field which are much stronger than the natural ones. The map of natural and technogenic magnetic fields with their applications and biological limits is shown in **Fig. 1.** A revolution in the medical technology endorsed the use of magnetic fields for biomedical applications such targeted drug delivery, magnetic hyperthermia, magnetic resonance imaging (MRI) and many others. A new scientific division, 'Magnetobiology', has been established to study the interaction of magnetic fields with living organisms[38]. In general, a magnetic field or magnetic energy is non-invasive in nature compared to electrical fields.. MNPs are primarily used in drug delivery, magnetic fluid hyperthermia, and for magnetic resonance imaging purposes in cancer theranostics..

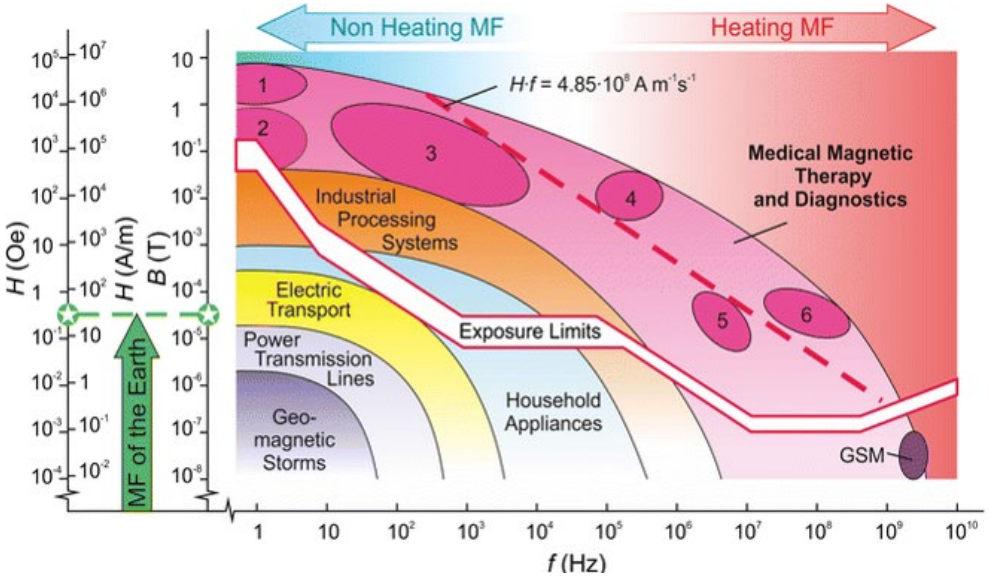

Fig. 1 The map of natural and technogenic magnetic fields currently used in medical sciences. Reproduced with permission from Ref.[37] Copyright © Springer Science+Business Media Dordrecht 2017.

A. Magnetically guided drug delivery

a. Underlying physics

MNPs can be used as a carrier to deliver drugs through the complex physiological architecture that includes blood, cells, and tight tissue junctions. These complicated trajectories can be modest in the presence of an AMF, and drag force experienced by MNPs is mostly due to the blood flow (**Fig. 2a**). Trajectory of the MNPs conjugated with drug molecules inside the body directed by an external magnetic field is represented by the equation[39];

$$Fm = \mu_0 VM.\nabla H \quad (1)$$

where, V is the volume of the material, μ_0 = 4π×10^{-7} N/A^2 is the magnetic permeability of vacuum, M is the magnetization (magnetic dipole moment per unit volume) and H is the applied (auxiliary) magnetic field. In order to effectively overcome the drag experienced by nano trajectory in the body, the magnetic force due to the external field must be greater than the inside drag force, and which is given by the equation;

$$F = 6\pi\eta r_h v \quad (2)$$

where, η is the viscosity of blood, r_h is the hydrodynamic radius of the particle and v is the velocity of the particles.

With the characteristics of driven magnetic accuracy, MF can be modulated externally in order to control the motion of nano-trajectory for high drug-carrying capacity and synchronized targeted drug release. Magnetically driven drug delivery platforms can therefore have lower toxicity and enhanced therapeutic effects. In principle, magnetic targeting and

stimulation in nanomedicine consists of the following steps (i) coupling the therapeutic drug to the MNPs (ii) applying an extracorporeal static MF to fascinate MNPs to the tumor or desired location; and (iii) the magnetically influenced drug release from the MNPs at a specific anatomic site under the extracorporeal alternating magnetic field (AMF). Extracorporeal static or dynamic magnetic fields can be positioned to improve the deposition of injected magnetically responsive drug carriers at tumour site, a process termed magnetic guidance. Physical basis of an MNP-based drug delivery system to targeted anatomical site such as a cancerous tumor is schematically represented in **Fig. 2b**. The typical setup for studying an *in vitro* AMF triggered drug release from iron oxide nanoparticles (IONPs) is shown in **Fig. 2c**. Researchers constructed a high power current generator feeding an application coil of sufficient diameter to hold the drug conjugated IONPs carrier sample (1–5 mL)[40].

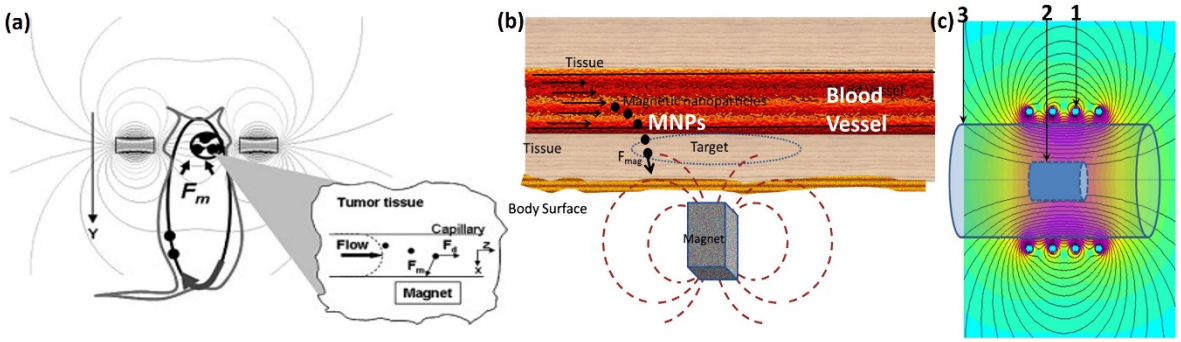

Fig.2 (a) Schematic illustration of brain tumor magnetic targeting following the systemic administration of magnetic nanoparticles. Targeting can presumably be achieved due to the combination of several phenomena including passive biodistribution of the administered nanoparticles, pathophysiological peculiarities of tumor vasculature and the principles of magnetic entrapment. Reproduced with permission from Ref[41]. Copyright © 2007 Elsevier B.V. (b) Schematic representation of a MNP-based drug delivery system to anatomical target site as cancerous tumor. Reproduced with permission from Ref[39]. Copyright © 2013 Elsevier B.V. (c) Setup for AFM triggered model drug release experiment through drug diffusion across semi-permeable membrane. 1: Solenoid and calculated magnetic field lines; 2: Dialysis bag (e.g. Spectra/Por Float-A-Lyzer™, 50,000 g mol^{-1} MWCO, 10 mm diameter, 5 mL volume); 3: Cylinder (50 mL) filled with aqueous buffer. Usually the drug is titrated in the outer medium, in "sink" and thermostatic (37 °C) conditions. Reproduced with permission from Ref[40]. Copyright © 2017 Elsevier B.V.

The efficiency of the magnetic guidance is dependent on the field effect expressed by MNPs under the force exerted on them by the EMF. The force acting on a single MNP exposed to an EMF can be calculated by modifying equation (1), and is given by the equation[42];

$$F_m = N.m.\nabla B \qquad (3)$$

where N = 1 (if N > 1 the force per an ensemble of N particles may arise), m is the magnetic dipolar moment and ∇B is the spatial gradient of the magnetic flux density. The fact that the magnetic force on an MNP cannot take a maximum magnitude within the body (away from the source of the magnetic field) means that, where the drug/particle complex is injected systemically, it is impossible to target regions deep within the body without targeting some

surrounding regions more strongly[43]. This underlying physical phenomenon behind the drug targeting leads us to conclude that the externally AFM targeted drug delivery of a nanosystem is appropriate solely for targets close to the surface of the body. However, within this limitation, such magnetic force driven tumor targeting would be more effectual compared with modest passive tumor accumulation of nanoparticles relying on the enhanced permeability and retention effect (EPR) of tumors.

b. Clinical progress

Inspired by the novel hierarchical design of hybrid nanostructures (HNCs) and their response to magnetic forces, diverse stimuli-responsive functional nanomaterials have been reported for drug delivery, involving various architectures and surface functionalities that respond to changes in magnetic fields[44–47]. In a few studies, it has been shown that the local temperature rise due to transformation of electromagnetic energy into heat (magneto-thermal response) is used to trigger changes in the HNCs without a need to elevate the temperature of the entire surrounding system[48–50]. Because of the abundant phenotypic diversity of cancerous tissues and solid tumors, drug targeting *via* the EPR effect are encountering set backs, and only a burst or "one shot" release may be envisioned in this case thus, limiting the chemotherapeutic outcome[51]. The HNCs coupled with a magnetic remote triggering modality ensure pulsatile spatiotemporal controlled cargo/drug release several times on demand, with control over the diffusion rates and the times of drug release. Using either uniform or non-uniform MF generated by an electromagnet with remote magnet positioning has been designed to strigger SPMNPs with a copolymer shell hosting the substrate and a complementary enzyme for cancer theranostics. These HNCs ~~are~~ consisting biocatalytic enzymes for triggering biocatalytic system to achieve well-controlled magnetic-field-triggered cancer drug release with a low strength magnetic field[50]. Although, this developed nanosystem is remotely activated under magnetic field, it is lacking the accurate control of on-demand repetitive drug release and rapid switching between "on" and "off" states. This has been further resolved by assembling a magnetic-driven drug delivery device called a 'microspouter'. This consists of a polydimethylsiloxane (PDMS) reservoir, a thin membrane, and a magnetic sponge[52]. Different from EPR drug targeting and release (diffusion-based) mechanism, the microspouter is driven by the magnetic sponge and can perform on-demand drug release instantaneously through a spouting triggered by external magnetic fields, *in vitro* and *ex vivo*. Distinct from targeted drug delivery, controlling ~~targ~~eting ratio is an essential factor for effective cancer nanotheranostics. This has been advanced by using magnetotatic bacteria as a drugcarrier. Magnetotactic bacteria

has been used to transport 70 different chemotherapuetic drug-loaded nanoliposomes into hypoxic regions of a tumour, to attain a high target ratio[53]. Each bacterial cell containsa chain of supermagnetic iron-oxide nanocrystals, and they tend to swim along local magnetic field lines and can possess magnetotaxis directional control towards a tumour. When operating in a computational algorithm and magnetic environment, this nanoassembly can rival artificial medical nanorobots/transporters of drugs in the tumour region with high targeting ratio.

To achieve a high yield drug release within the tumour microenvironment, a variety of nanoformulations have been designed to work in response to remote magnetic actuation., Liver tumours, for example, have been targeted with magnetic janus 'nano bullets'[54], pancreatic tumours targeted with magnetic microbubbles[55], colorectal cancer targeted with magnetic silica core/shell nanovehicles[56], and lung tumours targeted with hybrid peptide@magnetic nanoassembly[57]; all designed as remote magnetic actuation modalities. Ideal magnetic nanovechicles must satisfy a number of common criteria; specifically nanovechicles must (i) avoid *in vivo* non specific cellular intercations, (ii) faciliate high yield drug administriation at the tumour site away from the site of administration, (iii) enable elimination of nanocompunds from a tumour after its function as a carrier has been fulfilled. There are many ways in which these requirements could be fulfilled. For example nanomicelle SPIONs under magnetic drag force can deliver sorafenib drug (a pan tyrosine kinase receptor inhibitor and the sole chemotherapeutic agent clinically approved for hepatocellular carcinoma patients) to the tumour for systemic cancer therapy with high yield[58]. On the other hand magnetic single-walled carbon nanotubes[59] and superparamgnetic nanomicelles[60] can improve breast cancer and colorectal cancer immunotherapy, respectively, *via* magnetically driven drug delivery. These novel HNCs are efficiently delivering chemotherapuetic cargoes to tumour sites, while fulfilling the criteria stated above.

Instead of relying on conventional MNPs or SPMNPs involved in drug delivery strategies, the next generation of magnetic nanocapsules to treat tumours in a noninvasive way has been proposed (**Fig. 3**) [61]. State-of-the-art magnetic nanocapsules are designed to deliver chemotherapuetic cargoes with accurate control of (1) the release rate, (2) release amount, and (3) the number of doses, in an optimised magnetic field. Despite a number of attempts to magnetically guided drug delivery, this novel nanocapsule coupled with magnetic actuation resolving the issue of on-board drug components high yield.

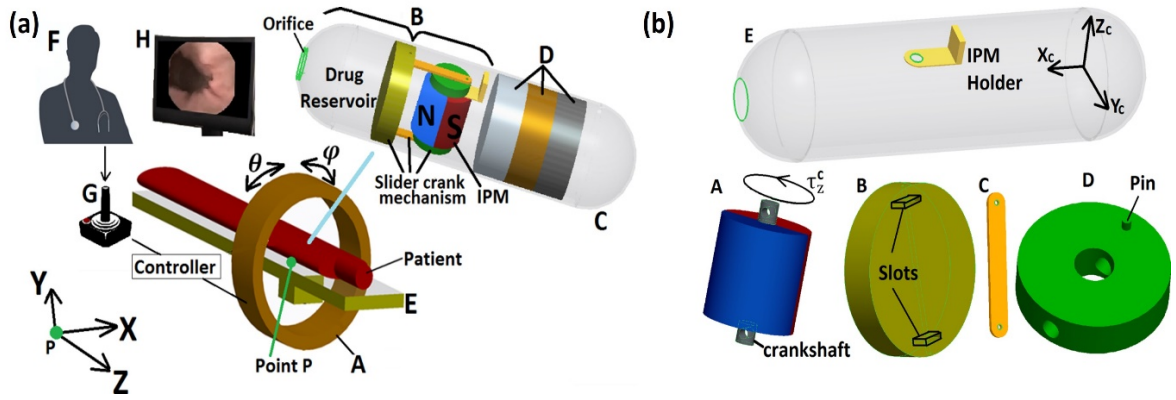

Fig. 3 (a) The main components of the proposed magnetic nanocapsule based drug delivery system. A: ring-shaped external magnetic system, B: drug release module, C: the robotic capsule, D: complementary modules within the capsule (anchoring mechanism, active locomotion system, and localization and orientation detection module), E: patient bed, F: clinician, G: joystick, and H: human capsule interface. Point P represents the origin of the general coordinate system XYZ, his taken with respect to the x-axis, and u is taken with respect to the z-axis. (b) The components of the slider crank mechanism. A: IPM, B: disk-shaped piston, C: connecting rod, D: disk, and E: robotic capsule. The coordinate system Xc Yc Zc of the IPM with respect to the general reference system XYZ is shown in Fig. (a). Image reproduced from Ref[61] copyright © 2016 by ASME.

To date, magnetically targeted nanosystems that use passive or active tumor targeting are lagging behind in clinical trials; all of the hybrid nanoassemblies currently being tested were only used for targeting or fixation after intravenous administration. The clinical practice of magnetic targeting is currently restricted by the limited depth of penetration, which is around 2 cm at present for SPIONs and other SPMNPs[46]. Effective ways to integrate magnetic guidance along with passive and active targeting is therefore a vital challenge, and needs to be addressed. Similarly, there is the potential to explore the utilization of the hyperthermic effect for treatment and controlled drug release, and MRI for diagnosis and monitoring. MNPs-based nanosystems have also been studied for MFH and MRI in pre-clinical trials, and are presented in the section below.

B. Magnetic fluid hyperthermia

a. Underlying physics

Though magnetic drag force has been used for targeting nanocargoes to a tumour site, their activation or therapy is the final step that completes nanotheranostics after reaching the target. Furthermore, AMF can also be used to release drugs from nanocarriers such as MNPs, liposomes or nanoemulsions. These nanocarriers can contain superparamagnetic nanoparticles (SPMNPs) that heat up to temperatures of the order of 42-45 °C under the influence of AMF and release drug to improve the outcome of cancer nanotheranostics[62,63]. SPMNPs have been extensively considered for remote controlled drug delivery applications where their response to static or AMF resulted in enhancement of the entrapped drug release rate within a tumor.

AMF at frequencies typically greater than 10 kHz has been used to remotely heat SPMNPs, and then, the local thermal fluctuations within the nanoassembly modulates drug releasing properties[64]. From a physical point of view, the presence of MNPs in an aqueous or physiological medium (considered as magnetically disordered medium) leads to extremely strong localization of the impact from the EMF and results in MFH therapy of the tumor. The main physical phenomenology related to MFH is the conversion of electromagnetic energy into heat when MNPs are subjected to AMF. The last decade has witnessed a significant increase in theoretical research related to MFH with emphasis on SPMNPs. The MFH is a novel approach that has been tested *in vivo*, to kill cancer cells at elavated temperatures of the order of 42-45 °C without damaging the surrounding normal tissues. MFH is a simplistic, yet realistic, radio-oncology methodology, however *a priori* estimation of the thermal history in internal tumours for optimizing a MFH treatment protocol for cancerious tumour is the need of the hour. Numerous review articles and book chapters have already dealt with the many facets of the physical aspects of MFH from its first phase to clinical transition. In this section, physical aspects standing in the way of more reliable MFH for clinical stage, mainly those published within the last few years, are discussed.

Without going into details of the dissipation processes of magnetic energy of MNPs and mechanisms of heat generation by these nanoparticles such as brownian motion, neel relaxation and hysterysis loss (schematics outlined in **Fig. 4**), the current section will outline the advanced biophysical mechanism of MFH. The physical mechanism of these processes has been thoroughly described in numerous reviews including recently in the same journal[65–68] ,and also by our group[69–71]. An ideal mechanism for MFH should be non-invasive, specific to the tumour cells, and enable precise targeting and localization to thedepth of tumor with utilising optimum thermal energy.. The computaional model of thermal energy dissipiation for tumor at the time of MFH therapy is designed to achieve focused cancer theranostics and is expressed in the classical Pennes bio heat equation[72];

$$\frac{\partial}{\partial x}\left(k_x \frac{\partial T}{\partial x}\right) + \frac{\partial}{\partial y}\left(k_y \frac{\partial T}{\partial y}\right) + \frac{\partial}{\partial z}\left(k_z \frac{\partial T}{\partial z}\right) + Q_{gen} - Q_b + Q_{met} = \rho C_p \frac{\partial T}{\partial t} \qquad (4)$$

This representative MFH temperature distribution model is taking care of 3-dimensional (3D) tumor anatomy and function of both space and time T(x, y, z). Q_{gen} is the volumetric heat generating source under MFH, Q_{met} is a metabolic heat generation by the physiological systems, and Q_b is heat removal by convective transport due to blood perfusion. This biophysical temperature modeling within tumor ensures further simplified solution,

isotropic thermophysical properties that are assumed for the tumour system. The average size of the tumor ranges from millimetres to centimetres and within this region the magnetic fluid is injected, and hence the order of magnitude for the effective tumour diameter undergoing MFH is ~10^{-3}. The thermal conductivity of tumour tissues is ~0.6W/mK at best that for water at room temperature, and the convective heat transfer coefficient due to cooling by the surrounding body fluid is similar to natural convective effects (heat transfer coefficient ~10 W/m^{2}K). Accordingly, the associated Biot number for the tumour is of the order of ~10^{-1} which satisfies the requirements of a lumped system modelling. Hence, Eq. (4) underlying the physics of MFH in tumor through energy balance between the transient thermal storage by the tumour and the heat generation due to MFH. Performance of the novel physical and computational predictions of the MFH compared with respect to the clinical trial report on murine systems by different authors has been validated[72]. The computational model derived for clinical MFH performs appreciably well with respect to the experimental data and more towards the later stages of hyperthermia.

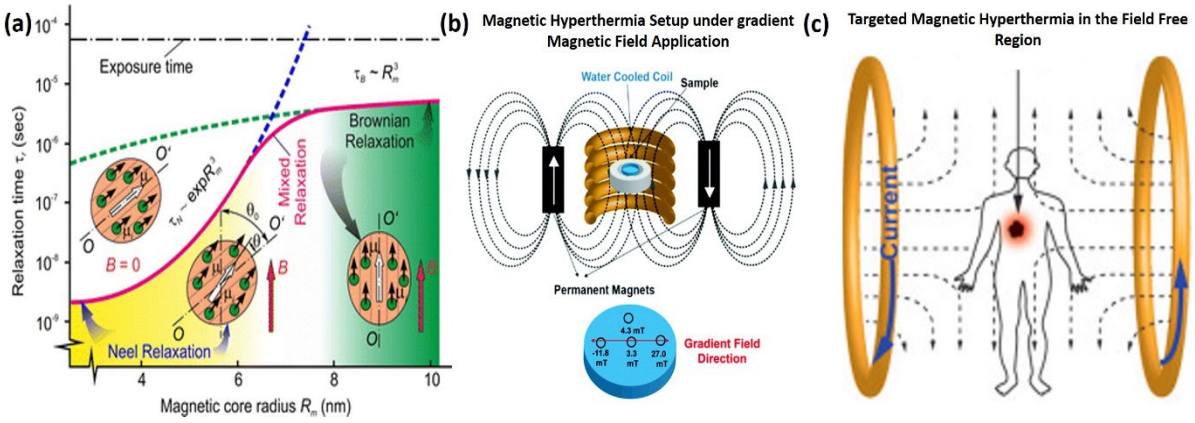

Fig.4 (a) Characteristic relaxation times of the MNP magnetic moments as a function of the magnetic core radius (for Fe_3O_4). O-O′ is the axis of easy magnetization, and μi and μ are the magnetic moments of the i^{th} atom and the nanoparticle, respectively. τ_N and τ_B stand for the time of Neel's and Brownian relaxation, accordingly. Exposure time is the half of the period of the sinusoidal AMF. Reproduced with permission from Ref[37]. Copyright © Springer Science+Business Media Dordrecht 2017. (b) Illustration of customized 3-D printed multi-welled sample holder with corresponding measured field strengths, and a schematic illustration of the magnetic hyperthermia measurement set-up under gradient magnetic field. Reproduced with permission from Ref[73]. Copyright © The Royal Society of Chemistry 2016. (c) Schematic representation of magnetic particle imaging (MPI)-guided hyperthermia treatment whereby the signal is generated in the field free region. Reproduced with permission from Ref[74]. Copyright © 2016 Chinese Materials Research Society and Elsevier B.V. T.

b. Clinical progress

Interest in MFH has grown immensely since it was first used in veterinary clinic to destroy metastases in lymph nodes in dogs in the year 1957. Since then countless efforts have been made to explore the potential of MNPs in cancer theranostics. In 1993, Jordan *et al*. directly delivered MNPs into a tumor for selective heating and found a much more effective hyperthermia therapy to kill cancer cells[75]. MFH is projected as a non-conventional cancer treatment modality based on the physiological circumstances of tumour cells; usually cancer cells possess higher heat sensitivity over normal cells at milder temperatures bordering 43 ºC, resulting in damage to tumor cells only[76]. Depending on the treatment modality and location tumors are typically heated in the range of 41–46 ºC (moderate hyperthermia) or >46 ºC (thermoablation) for a definite time interval. MNPs can magnetically target a tumor site following intra-tumoral, intra-peritoneal, intra-arterial, intra-cavitary, or intravenous administration (**Fig. 5**). However, oral administration of MNPs is inappropriate as most of the MNPs will be fecally excreted, owing to their large size[77].

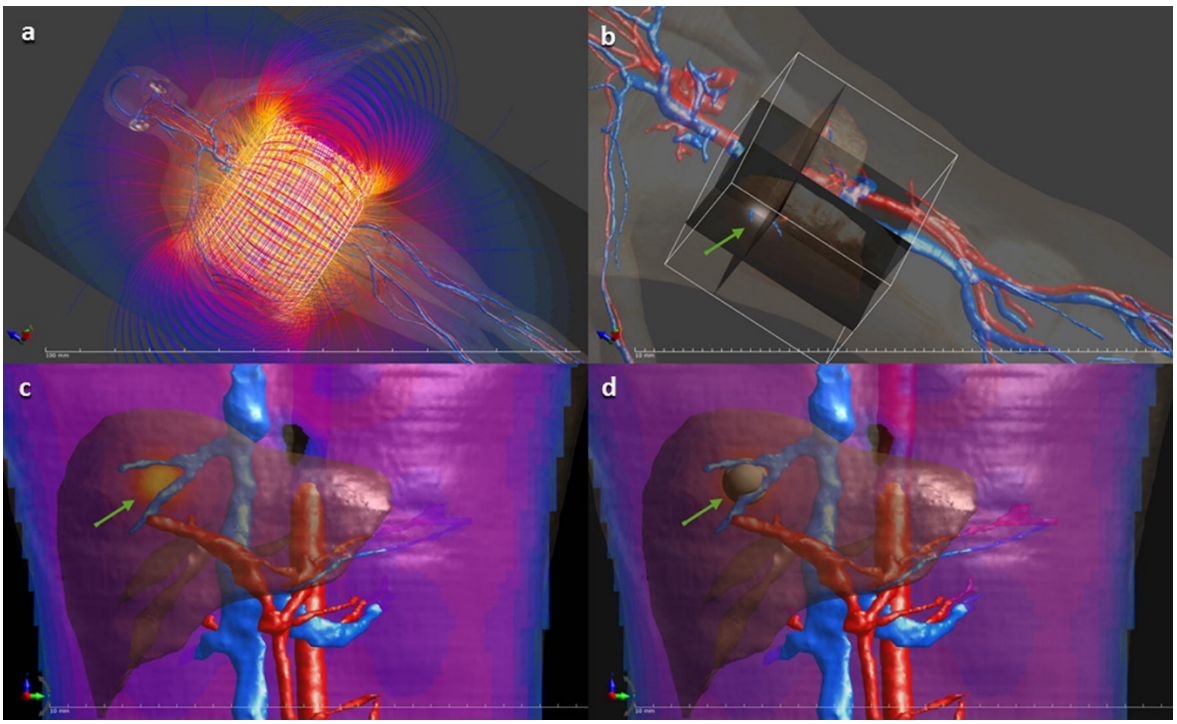

Fig.5 Next generation MFH therapy coupled with nanotheranostics at clinical stage and modelling of MNPs-based hyperthermia therapy: (a) simulated magnetic field generated by a coil applicator; (b) image-based particle density in the liver; (c) induced tissue temperature distribution considering perfusion and major vasculature; (d) resulting ablation as determined using CEM43 thermal dose model. The targeted tumour location is indicated with an arrow. Reproduced with permission from Ref[78]. Copyright © 2016 Elsevier Ltd.

For pre-clinical or clinical MFH applications it is crucial to accurately control temperature and magnetic fluid concentration in and around the target volume. Tumor

temperature rise is mainly dependent on cancer tissue properties such as blood perfusion cooling, and specific absorption rate (SAR) of homogeneously dispersed MNPs within the tumor. A recentstudy showed that a bladder catheter could be used to inject MNPs into a bladder tumor [79]. A homogenous dispersion of a magnetic nanofluid containing IONPs was injected into a bladder tumor and monitored using MRI. Uniform power dissipation within the bladder target was achieved using this novel nanotheranostic technique. A preclinical MFH investigation using a novel small animal MF applicator on 25 female rats with bladder cancer showed well-localized heating of the rat bladder lumen with effective control of temperature in the bladder, and minimal heating of surrounding tissues. On the contrary, hybrid engineered magnetic thermo-responsive iron oxide nanocubes are designed to merge MFH and heat-mediated drug delivery at preclinical stage[80]. This nanotheranostics platform works under clinical MFH coupled with MRI and at a low iron dosage. The platform is enabling translation of MFH mediated chemotherapy and the ability to monitor tumour progression post-MFH-treatment by MRI, thus overcoming the clinical limitation of MFH. After promising results *in vitro*, the nano-therapeutic system must be assessed *in vivo* before entering the clinical stage. Several recent studies reporting *in vivo* experiments confirm the ability of various hybrid MNPs/SPMNPs entities to eradicate different tumours such as breast, liver, colon etc., completely via MFH[81–84]. The MFH modality offers a unique advantage in brain cancer therapy as well, in that it can non-invasively and remotely induce tumor suppression *via* mechanical force of MNPs[85]. AFM with low frequencies can penetrate the human head, without damaging the normal brain tissues and can be operated in a time selective and spatially constrained manner for remotely triggered nanotheranostics, as the interaction is mediated by the MNPs[86].

Next generation HNCs accommodating MNPs inside a liposome bilayer in a single nanoplatform, termed “magnetoliposomes”, have recently been introduced into cancer theranostics[87–90]. Well-defined temperature kinetics and controlled drug release is mandatory to improve the efficacy of MFH. Magnetoliposomes can suffer changes in their assembly and permeability and release their payload in a controllable way by partial disruption of the bilayer structure under AFM pulses or heat produced by MFH. The thermo-responsive behavior of liposomes is broadly customized close to the clinically relevant hyperthermia values. In recent research work, short magnetic pulse (500 kHz, 20 kA) thermosensitive bilayer-embedded magnetoliposomes were proposed to enhance MNPs mechanical motion induced drug release in the HeLa tumor model and MFH without distressing normal cells by overheating[91]. These novel HNCs combine magnetic targeting as well as active targeting modality (methotrexate as

a surface ligand for folate receptor-overexpressed cancer cells) with DOX and a fluorescent dye (Cy5.5) for tumor imaging, and achieved 100 % tumor suppression within 14 days.

In recent years, MFH has been suggested as localized therapy to heat a specific region of the body, e.g. a tumor. In order to improve the effectiveness, MFH has often been evaluated as an adjunct therapy to enhance chemotherapy and radiotherapy., MFH, for example, can synergistically enhance the efficacy of numerous chemotherapeutic drugs including doxorubicin, cisplatin, cyclophosphamide and bleomycin[77,92,93]. Apart from chemotherapy, MFH can also improve radiotherapy by enhancing the thermal enhancement ratio (TER), where TER is the ratio of the dose of radiation alone that is required to achieve the end point to the dose of radiation with heat to achieve the same end point[94]. MFH is believed to boost radiotherapy outcome *via* protein denaturation following inactivation of proteins involved in DNA repair. *In vivo*, MFH can increase vascular perfusion and oxygenation of formerly radioresistant hypoxic areas, leading to radiotherapy success. There have been a number of incremental *in vivo* pre-clinical trials in recent years on the impact of MFH on various cancers in combination with radiotherapy, chemotherapy, or both, using various HNCs[94–96]. This contribution emphasises the potential utility of MFH to exploit non-localised effects, and different approach to avoid issues with targeting NPs heat deposition, opening the possibility to explore novel directions for nanotheranostics[97].

Although MFH has been integrated into clinical practice to treat a relatively wide range of cancer types, it is necessary to consider some clinical fundamentals when locally dealing with solid tumors: (i) The penetration depth of AMF should be higher, allowing to reach deeper tumor tissues, (ii) MNPs administration in tumor site in a wide concentration range and continual throughout the MFH treatment for repeated therapy sessions, (iii) The heat generated should be uniform within the tumor microenvironment and it must be the highest possible at the lowest particles dose, (iv) Reliability for providing a precisely controlled intra-tumoral heat exposure mediated by MNPs[68],(v) Safety of AMF to human body and vital organs including high voltages producing eddy currents in physiological media. Another main concern relates to the safe use of AFM for whole body or tumor only. Recent reports proposed that to protect healthy tissue surrounding the tumor against excessive heating, the product of applied field amplitude and frequency (*Hf = C)* must be limited ($C \leq 4.85\times 10^8$ A m^{-1} s^{-1}). There are two different approaches for the application of AMF in the clinic. The first is that the theoretical limit of $C \leq 4.85\times 10^8$ A m^{-1} s^{-1} is for whole-body exposure. The second is that this criterion will be accordingly weaker for smaller body regions being under field exposure. For instance,

a combination of field amplitude of about 10 kA m^{-1} and frequency of about 400 kHz (leading to $Hf = 4\times 10^9$ A m^{-1} s^{-1}) was suggested for the localized treatment of cancer[98,99].

MFH has shown to be a promising approach to overcoming the barriers encountered by current cancer therapies in the last decade. Since then significant efforts have gone into the development of clinical MFH trials together with nanotheranostics. The publicly listed company MagForce AG, based in Germany, has developed different hybrid nano assemblies such as aminosilane coated ferrofluid (NanoTherm®), an AMF applicator device (NanoActivator®), and temperature simulation software (NanoPlan®). In recent years the company has successfully conducted Phase 1 and 2 clinical studies on glioblastoma and prostate cancers patients using intratumorally delivered MNPs and application of AMF *via* the proprietary MagForce system[66]. In the Phase 2 clinical trial conducted by MagForce patients with recurrent glioblastoma demonstrated a median overall survival of 13.4 months (n=66) from the time of tumor recurrence. During and after the MFH treatment, treated patients showed no prolonged side effects other than worsening motor disturbances, which may be related to disease progression rather than MFH. In the Phase 1 and 2 trials MagForce is using lower frequencies of 100 kHz, and a field strength of 1.35×10^9 A m^{-1} s^{-1} to 8.5×10^8 A m^{-1} s^{-1} for glioblastoma patients, whilst for patients with prostate cancer 5×10^8 A m^{-1} s^{-1} is used.

C. Magnetic imaging

a. Underlying physics

1. Magnetic Resonance Imaging

One of the holy grails in cancer theranostics is to achieve accurate diagnosis and imaging of tumor boundaries. Multimodal imaging strategies incorporating diverse images have increased the ability of oncologists to diagnose, guide, and monitor outcomes of cancer therapy. MRI is an extensively used radiological/biomedical imaging technique and can facilitate multi-parameter anatomical demonstration of diagnosis[100]. The development of biomedical instrumentation and the use of contrast agents has provided better-quality tumor imaging. However, the issue of accuracy and false imaging remains a problem[101]. MRI is both ionizing radiation free and non-invasive , and that permits reconstruction of an atomic nuclear magnetization signal into two-/three-dimensional (2D/3D) images. The underlying physical phenomenon of MRI in clinical translation is to acquire the restored or residual magnetization by adjusting parameters in either the longitudinal direction or the transverse plane (**Fig.6**). The longitudinal imaging or spin lattice relaxation parameter is termed T_1-weighted MRI, and the transverse or spin-spin relaxation parameter is termed T_2- weighted MRI. Basically, T_1 and T_2

images show bright and dark signal contrasts, respectively, which represent recovered (T_1) or residual (T_2) magnetization after a specific time cycle. Usually, T_1 MRI is advantageous for assessing fat tissue or liquid retaining anatomical assemblies (e.g., joints), which are challenging by T_2 MRI. In contrast, T_2 MRI is powerful in assessing water-rich anatomies, which appear as bright signals in specified spin-echo (SE) sequence. SE protocol or arrangements is useful for T_1- or T_2-weighted contrasts and helps in creating molecular interplay by removing effects of exterior magnetic fields.

The main shortcoming of MRI is the contrast image generated is not enough for an accurate tumor diagnosis. Despite the fact that the proton density of a tissue is stationary, enhancing the signal quality or modifying the relaxation time by administering a contrast agent can alter the magnetic characteristics of nearby water protons. The signal enhancement due to a contrast agent depends on its longitudinal (r_1) or transverse (r_2) relaxivities, which are defined as the increase of relaxation rates $R_1=1/T_1$ and $R_2 =1/T_2$, respectively[102]. The use of paramagnetic metal ions as MRI contrast agents has made a significant impact by influencing the MRI signal properties of surrounding tissues. Gadolinium-based metal oxides extensively used as MRI contrast agents in cancer, cardiovascular, and inflammation diseases. SPMNPs present great advantages as T_1-T_2-weighted contrasts agents over the gadolinium-based oxides as they possess suitable magnetic saturation and superparamagnetic properties, which are crucial for enhancing MRI signals and contrast.

The efficacy of a MRI signal intensity without and with contrast agent including SPMNPs is evaluated by the following equation:

$$R_i = \left(\frac{1}{T_{i,0}}\right) + r_i C \tag{5}$$

where R_i is the observed relaxation rate (s^{-1}); $T_{i,0}$ is the relaxation time before adding the contrast agent (s), r_i is the relaxivity coefficient ($mM^{-1}\ s^{-1}$), and C (mM) is the contrast agent concentration. Superparamagnetic iron oxide nanoparticles (SPIONs) with diameters of several nanometer, which can be detected by high magnetic field, have also been studied as T_1 and T_2

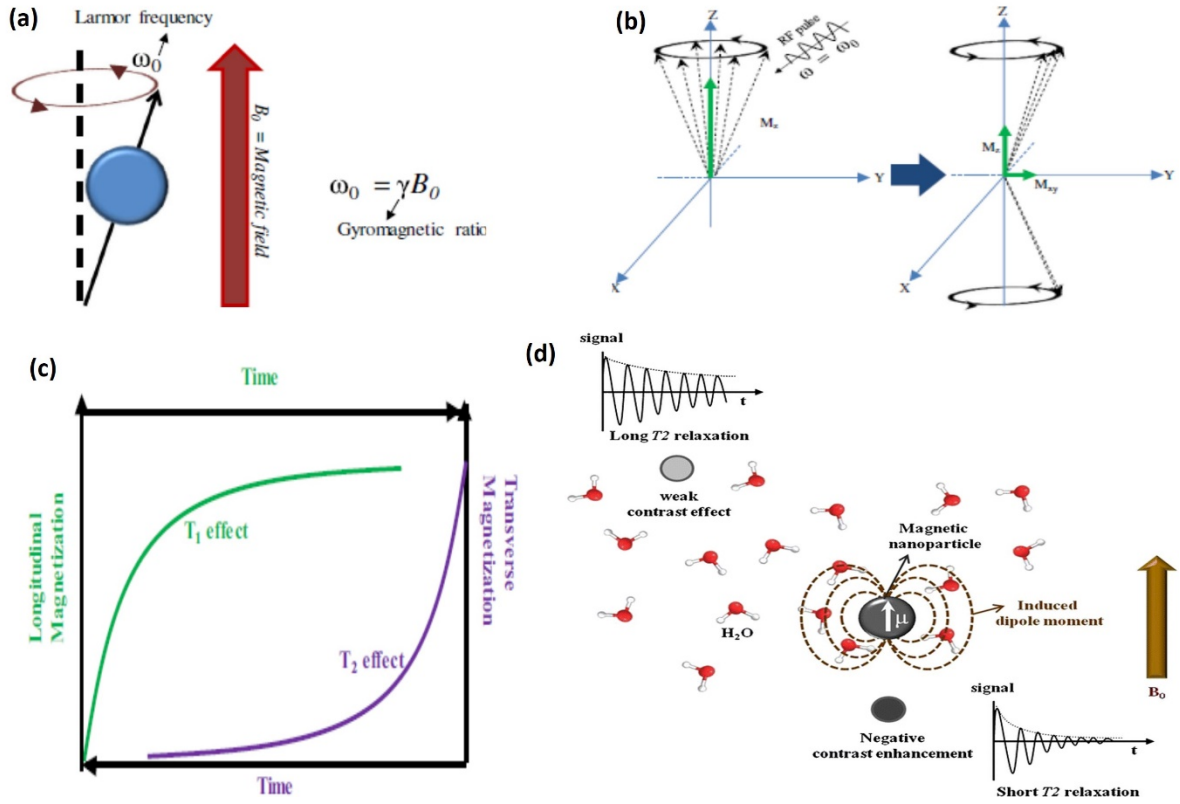

Fig. 6 Schematic summary of MRI principle using IONPs. (a) Alignment of spins under applied magnetic field B_0 and precession under Larmor frequency ω_0. (b) Spin relaxation mechanisms of T_1 and T_2 after applying Radiofrequency (RF) pulse. (c) Hypothetical graphs of longitudinal and transverse relaxation with time. Reproduced with permission from Ref[103]. Copyright ©Springer Science+Business Media B.V. 2017 (d) Illustration of the contrast enhancement of magnetic nanoparticles. Under an external magnetic field, magnetic nanoparticles generate an induced magnetic dipole moment that perturbs the magnetic relaxation of water protons. Such changes result in signal reduction on T_2-weighted MRI and lead to MR contrast enhancement, with darkening of the corresponding section of the image. Water protons influenced by magnetic nanoparticles have relatively short T_2 relaxation and produce negative contrast enhancement. Reproduced with permission from Ref[104]. Copyright © Controlled Release Society 2011.

contrast agents, being capable of visualizing individual cancer cells. The high magnetic susceptibility of SPIONs enables them to be identified as darker signals on the MRI images being suitable T_2 contrast agents. The T_2 relaxivity for SPIONs is at least 5–10 fold higher than T_1 relaxivity. Recently our group introduced the primitive concept of dual-mode contrast agents by making hybrid gadolinium doped SPIONs[105,106] for cancer theranostics. According to outer-sphere spin–spin relaxation approximation, the relationship between the magnetization and the T_2 relaxation rate (R_2) for SPMNPs is described by equation[107];

$$R_2 = \frac{1}{T_2} = \frac{256\pi^2\gamma^2}{405} m_s^2 V \times \frac{r^2}{D(1+\frac{L}{r})} \quad (6)$$

where γ is the gyromagnetic ratio of the protons, m_s is the saturation magnetization of the MNPs, V is the MNPs volume fraction, r is the MNPs radius, D is the diffusion coefficient of

water molecules, and *L* is the thickness of the surface coating. From equation 6 we can observe that the T_2 relaxation rate (R_2) is dependent on the m_s value. Given that the magnetic properties of the SPMNPs are dependent on physicochemical parameters, such as size and composition and can be easily tuned by controlling these, it is possible to develop SPMNPs with large m_s values to achieve high T_2 contrast effects. In contrary to T_2, T_1 contrast effects are the result of magnetically disordered spin layers at the surfaces of the MNPs. The metal ions at the NPs surface has a number of unpaired electrons, for example Fe^{3+} have 5 unpaired electrons, that in entirely accelerate the T_1 relaxation process. However, high magnetization of MNPs with high r_2 and r_2/r_1 values are inadequate for T_1 contrast agents. Broad r_1 while decreasing r_2 and r_2/r_1 values is the ultimate solution for improving T_1 contrast effect, this can be possible with increasing the share of canted surface spins of MNPs by decreasing the size of the MNPs. Theoretical investigation suggested that the optimum size of MNPs should be smaller than 10 nm to achieve strong T_1 contrast effects[107].

2. Magnetic Particle Imaging

The use of MRI and contrast agents in cancer theranostics has a long history. MRI provides quality imaging of tumor and information for theranostics, but for more accurate tumor

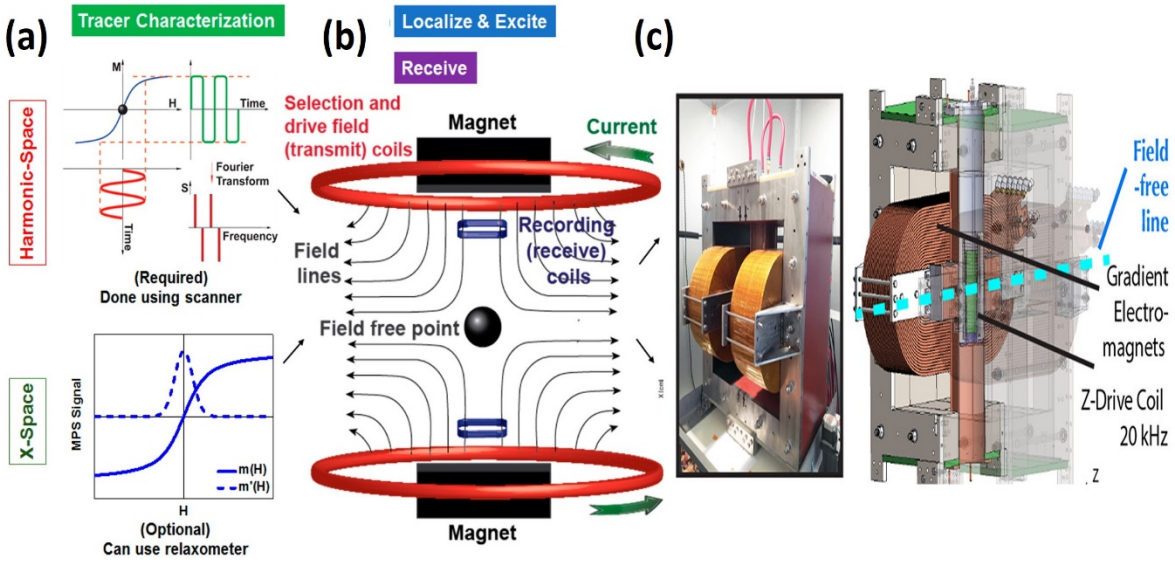

Fig. 7 Schematic representation of the MPI image generation workflow, comparing harmonic-space and x-space MPI. The MPI image generation process can be divided into four steps: (a) tracer selection and characterization, (b) excitation and spatial localization and signal reception. Reproduced with permission from Ref[108].Copyright© 2015, American Chemical Society. (d) Hardware setup of the MPI scanner designed at

Department of Bioengineering, University of California at Berkeley. Reproduced with permission from Ref[109]. Copyright© 2018, American Chemical Society.

diagnosis, a higher resolution, real-time *in vivo* imaging and monitoring is required. In particular, tomographic imaging, has become a radical tool for visualizing tumor lesions, showing selectivity of diseased and normal tissues, and monitoring blood flow in the human body. The magnetic particle imaging (MPI) technique discovered by Gleich and Weizenecker at Philips Research Laboratories in Hamburg, evolved into a tomographic imaging method for high spatial and temporal resolutions of tumors[110]. MPI is driven by the physics of its tracers, which are typically MNPs or SPIONs. The MPI signals rely on the nonlinear re-magnetization response of SPIONs to an oscillating MF. If MNPs (typically SPIONs) are exposed to an oscillating MF with frequency (f_1) and amplitude (A), the MNPs will exhibit a magnetization $M(t)$, where t is time. The relationship between the AMF and the resulting magnetization $M(t)$ is nonlinear. At this stage, the MNPs can either undergo a Brownian rotation (physical particle rotation) or Neel rotation (internal magnetic moment rotation).These relaxation properties of SPIONs in the presence of an AMF afford the foundation for signal generation and acquisition in MPI[111]. Since the relationship between the AMF and the resulting magnetization of SPIONs is nonlinear, this leads to harmonics in the detected signal (**Fig. 7**). These produced harmonics can then be used to quantify the local concentration of the SPIONs by a simple Fourier transform as illustrated in the equation below[111];

$$S_n = Fourier\,\{u(t)\}; u(t) \propto -cdM(t)/dt \quad (7)$$

where *Sn* is the SPIONs harmonics, u is the voltage signal measured in the receive coils, c is the concentration of the SPIONs, and M is the magnetization of the SPIONs. The generated higher order harmonics for a nonlinear magnetization curve can be further mathematically expressed by expanding the Langevin function into a Taylor series[111]. After the raw data or signals captured for MPI, reconstruction algorithms are used to facilitate the conversion of signals into images. Two principal methods of image reconstruction techniques have been reported to date: harmonic-space MPI, and x-space MPI. The physics of these techniques is underlined in recent review articles and book chapters[108,112,113].

b. Clinical progress

Advancements in nanotechnology over the last three decades have led to the development of novel magnetic imaging modalities for cancer theranostics. Owing to the need

for precise imaging of tumor boundaries in complex environments, new MNP based multimodal imaging techniques are in progress. The HNCs (including various type of bare and functionalized MNPs) studied over last decade allow multi-modality to overcome the inherent instrumental limitations of magnetic imaging systems for tumor imaging. In particular, MNPs are used to improve sensitivity, resolution and accuracy of the magnetic imaging modalities. Over the years, various synthetic, structural, physicochemical and magnetic imaging aspects of nanomaterials have been discussed in a number of excellent reviews[103,114–116]. Here, we summarize the updated state-of-the-art clinical research on HNCs developed for magnetic imaging in cancer theranostics (including therapy monitoring by MRI and MPI). While previously discussed issues like MRI contrast enhancement, NPs physical and chemical parameters, preliminary *in vitro* and *in vivo* studies, etc., will not be covered in the present section.

The Next generation multimodal-imaging nanoprobes offer a novel approach, which can provide detailed diagnostic information for the planning of image-guided diagnostics and therapy including surgery monitoring, *via* the application of biocompatible nanomaterials integrating MRI in clinical practice. In recent time, catheter-directed hybrid magnetic microspheres based drug delivery and MRI-guided cancer nanotheranostics approaches has been proposed to treat cancer effeciently[117]. This approach offers cancer patient-specific

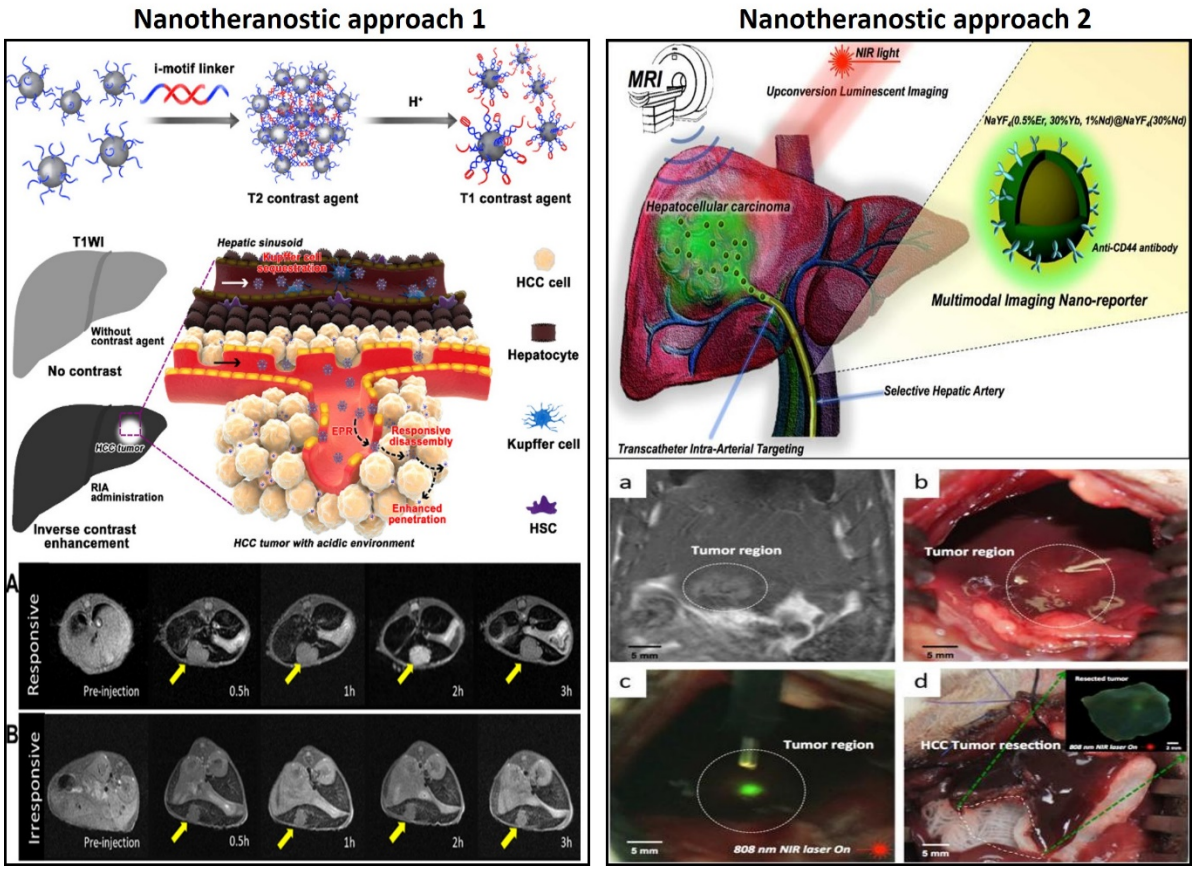

Fig. 8 MRI guided cancer nanotheranostics approaches. Approach 1: designing HNCs with DNA-modified ultra-small iron oxide nanoclusters (USIONCs) cross linked by pH-responsive linker DNAs to fabricate the responsive iron oxide nanocluster assembly (RIA). Upon intravenous injection, RIAs are routinely sequestrated by Kupffer cells in liver, whereas they disassemble into dispersed USIONCs when extravasated in the acidic HCC tumor environment. Under T_1-weighted MR imaging(T_1WI), the normal liver appears dark due to the presence of RIAs, while the HCC tumor becomes bright by the USIONCs. Schematic of multimodal MR/Upconversion luminescent imaging of HCC tumor using transcatheter hepatic intra-arterial. Panel 2 Clinical small HCC diagnosis by RIAs. (A) T_1 weighted images RIAs and (B) IRIAs in orthotopic HCC mice. Reproduced with permission from Ref[118]. Copyright © 2018 American Chemical Society. Approach 2: Schematic of multimodal MR/Upconversion luminescent imaging of HCC tumor using transcatheter hepatic intra-arterial (IA) targeted anti-CD44-Nd-CSUCNPs. Next generation multimodal diagnostic MR and intraoperative Upconversion luminescence (UCL) image-guided surgery for HCC resection was demonstrated. Panel 2 (a) MR T_2 weighted images of rats after IA delivery confirming HCC detection of anti-CD44-Nd-CSUCNP imaging reporters, (b) digital imaging of HCC lesion, (c) detection of HCC with UCL imaging of IA targeted anti-CD44-Nd-CSUCNPs and NIR light (808 nm), (d) an image of liver after image-guided hepatic electro-cauterization resection, (inset) UCL imaging of resected HCC tissue with NIR light (808 nm).

personalised medicine, that permit dosimetry and tumor-specific treatment of liver tumor with reduced systemic toxicity and superior therapeutic effect. Researchers from the Center for Nanomedicine, Institute for Basic Science (IBS) Seoul, Republic of Korea introduced distance-dependent magnetic resonance tuning (MRET) for the noninvasive exploration of a wide range of biological events in deep organs including tumor[119]. To demonstrate this nanotheranostics potential, a three component system was developed, enclosing paramagnetic enhancer Gd-DOTA core with superparamagnetic quencher (12 nm $Zn_{0.4}Fe_{2.6}O_4$ NPs) and a thick layer SiO_2

(~ 18 nm). The enhancement of T_1 MRI signal is obtained at the tumor region, providing high-resolution anatomical information and soft tissue contrast without a penetration depth limit which is difficult to achieve with current optics-based approaches.

Existing MRI modalities coupled with contrast agents rely on single-phase contrast enhancement of tumor, which is not sensitive enough to detect and monitor early stage small hepatocellular carcinomas (HCCs), especially those less than 1 cm in size. Diagnosis accompanied by timely curative monitored treatments of these small early stage HCCs can increase the median 5-year survival rate of patients from 5% to over 50%[118]. Two different versatile MRI based nano-platforms are proposed by different research groups (**Fig. 8**). The first approach was based on an intelligent MRI contrast agent, termed responsive iron oxide nanocluster assembly (RIA). This was fabricated by linking iron oxide with i-motif DNA-derived pH-responsive linkers[118]. The HNCs shorten the transverse relaxation time and the initiation of MRI modular switch from T_2 to T_1.. A second nano-platform deals with developing Lanthanide-based upconversion MNPs (UCNPs) to serve as multimodal-imaging reporters providing tumor-specific detection, surgical intervention and image-guided surgery for resection of HCCs[120]. Compared with T_2 or T_1 (‘‘turn-on’’) contrast enhancement, designing T_2–T_1 switching contrast agents are usually more desirable for accurate tumor diagnosis at clinical stage. These next generation contrast agents enable ‘‘brightening’’ imaging with high sensitivity and signal-to-noise ratios. Yang and his research group from Shanghai Normal University have reported Fe_3O_4-based T_2–T_1 switching MRI contrast agent for distinguishing between normal tissue and tumor tissue *in vivo*, by utilizing pH- and GSH-responsive ZIF-8 (Zeolitic imidazole frameworks) as a matrix[121]. In preclinical stage novel HNCs show T_2–T_1 weighted switching in mice liver sites and enhanced contrast darkening. The tumor sites exhibited darkening to brightening contrast enhancement, giving larger inverse contrast for differentiating the normal tissue and tumor tissue boundaries. Over the past few years, various novel HNCs have been proposed in cancer nanotheranostics to guide therapy using MR and computed tomography (CT) imaging. This includes magneto-plasmonic NPs in Brain cancer[122], silica coated metal chelating-melanin NPs in protest cancer[123], and hybrid iron oxide nanocubes for natural immunotherapy of liver tumor[124].

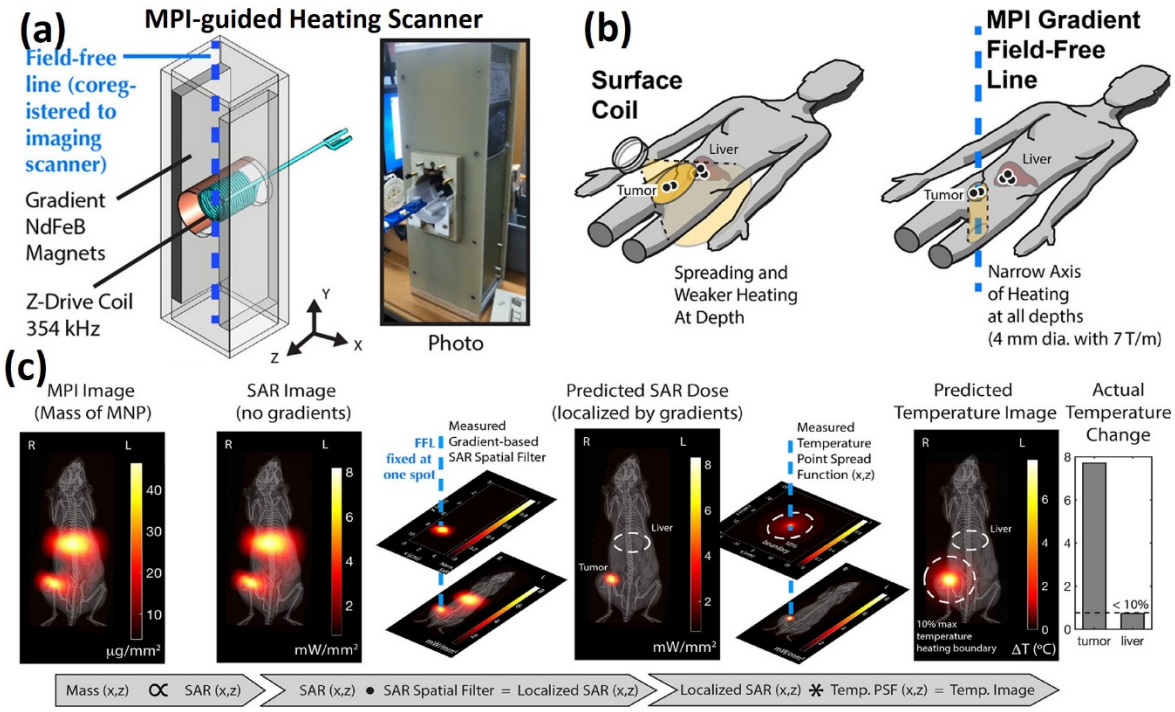

Fig. 9 MPI guided MFH cancer therapy in clinical stage. (a) Setup of the MPI scanner and the image-guided magnetic hyperthermia scanner. (b) Illustration of MPI-localized heating in the tumor while sparing the liver. Experimental demonstration that MPI can predict the spatial distribution of heating for image-guided, gradient-localized magnetic hyperthermia. Reproduced with permission from Ref[109]. Copyright©2018 American Chemical Society.

In clinical instances numerous cancerous tumors are not easily accessible or amenable to surgery and radiotherapy but can be reachable to magnetic field and thus, MFH combined with MPI could perhaps be more effective and appropriate. The next generation cancer nanotheranostics

often involves cancer-targeting SPIONs administered intravenously for MPI followed by MFH. The MPI can monitor blood flow to the tumor *via* SPION tracers and could assess the efficacy of the treatment as well as monitoring metastasis through sentinel lymph nodes. MFH can further reduce the burden of aggressive tumor progression by suppressing cancer cell resistance to chemotherapeutic drugs. A proof of concept was demonstrated in a preclinical setting by Hensley *et al.*, 2017[125]. Simulation and experimental work was carried out to quantify the extent of spatial localization of MFH using MPI systems. Combined MPI-MFH system performed on-demand selective heating of MNPs samples separated by only 3 mm (up to 0.4 °C s^{-1} heating rates and 150 W g^{-1} SAR deposition) allowing for spatially selective heating deep in the body and generally providing greater control and flexibility in MFH. This novel nanotheranostics approach was further clinically validated by Tay and coworkers, 2018[109]. The research group demonstrated a nanotheranostics platform, with quantitative MPI

image guidance for treatment planning and use of the MPI gradients for spatial localization of MFH to arbitrarily selected regions of the liver tumor while minimizing collateral damage to the nearby liver (1-2 cm distance). Apart from localizing cancer therapy, the system can be extended to localize actuation of drug release with high contrast and high sensitivity imaging combined with precise control and localization of the actuated therapy. Clinical experimental data validated that the MPI-MFH theranostics platform can selectively heat tumors separated by 7 mm with negligible heating of off-target sites, by delivering SPOINs to the target site (**Fig. 9**). There is growing interest to further develop the field of cancer nanotheranostics combined with MPI[126]. Biomedical engineers are designing MPI clinical machine/techniques for improved acquisition and reconstruction[127]. At present, we are at the very beginning of exploring MPI-MPH in cancer therapy, with optimal instrumentation, SPIONs, and image formation in place, it will be the time for oncologists, biomedical engineers to take MPI-MFH to the next generation for discoveries in cancer nanotheranostics.

D. Future opportunities and challenges

These are indeed very exciting times for the development of magnetically stimulated cancer nanotheranostic systems with different MNPs/SPIONs/SPMNPs as carriers. The current step of technological advancement gives the impression of further progress in the clinical development and that should be a goal in the near future. Although clinical translation of magnetically stimulated cancer nanotheranostics is still in its first phase, scientist working on the development of this emerging technology anticipate it will compete strongly with other modalities now routinely used in disease diagnosis. The most exciting aspect of magnetically induced theranostics with various types of MNPs is their potential to be equipped with many spatial therapeutic effectors, with a selective external control. However, even at this median stage, when first-hand novel concepts and strategies for MF based external release systems are only beginning to be realized in pre-clinical tests, it is important to focus on the potential and relevance of these technologies in the clinical oncology. Magnetically triggered nanotheranostics modality is advantageous to address important shortcomings of current cancer therapies based on nanotechnologies for example; (i) direction of NP carriers to tumor tissues with precise external control deep within the human body, (ii) triggered release of chemotherapeutic cargo at this depth with precise remote control, (iii) MFH promote bursting elimination of the tumor tissues without off-target effects and without the possibility of tumor reoccurrence,(iv) image guided cancer therapy preprocedure planning and identifying tumor volume, (v) magnetically guided catheters promoting intra procedural tumor targeting, (vi) MPI

is advancing state of the art of tumor monitoring before and after the treatment, (vii) intraprocedural and postprocedure treatment control assessment such as measuring effectiveness for further intervention. The real present-day challenge in the design of such a novel technology is related to a concerted effort from specialists in each field such as physics, spectroscopy, chemistry, biology, medicine and oncology. The other limitation is linked to HNC development towards maintaining biocompatibility as well as combining multiple magnetically induced release mechanisms. A major challenge for novel HNC design is to prevent mineral leaching from the inorganic core and organic shell and permit clearance from the body in an appropriate timeframe.. Furthermore, achieving a 100 % therapeutic effect without damaging surrounding healthy tissues is the challenge of MFH therapy. Finally, addressing each of these shortcomings requires a concerted effort from nanotechnologists and clinicians.

IV. Light-Stimulated Nanotheranostics

The use of light in modern medical practices was began in the late nineteenth century. The physician Niels Finsen, was awarded the Nobel Prize in Physiology and Medicine in 1903 for phototherapy based on ultraviolet (UV)-induced treatment of lupus vulgaris. This fundamental light–matter interaction discovery lead to swift improvements in the understanding of light in medicine to diagnose, and cure various diseases. The light, or photons, interact with biological tissue and biological matter via various processes for example scattering and absorption of light within tissues. This is summarized in (**Fig. 10a**). Since the discovery of the laser in 1960, new medical avenues have been opened for biomedical engineers and clinicians. Today, lasers are routinely used in medical applications, including eye surgeries, cutaneous disorders, and tumor tissue ablation through fibre-optic delivery. Recent advances in optical technologies and biomedical engineering have enabled biomedical devices; in particular, those that coupled nanotechnology with photonics and laser. This has led to a global market for therapeutic lasers estimated to be over US$3 billion[128].

Since nanotheranostic integrated into one entity is executing multiple functions, modalities with different functions, multiple light-triggered functions could be easily integrated into one single nanoplatform. This multifunctionality in a well-defined pattern through elegant but feasible construction is challenging for a conventional molecular design and synthesis perspective[129]. Light-induced cancer nanotheranostics are normally responsive to ultraviolet (UV), visible (Vis) and near infrared (NIR) light, although this is heavily dependent on the properties of nanomaterials. For instance, commonly reported organic and inorganic

photosensitizers (PSs) zinc phthalocyanine (ZnPc), indocyanine green (ICG), zinc oxide (ZnO), titanium oxide (TiO_2) quantum dots (QDs), are responsive to UV, Visible or NIR light, and are used in photodynamic therapy (PDT). Moreover, polyaniline (PANI), polypyrrole (PPy), gold (Au) nanorods, $Cu_{2-x}S$ NPs, nano reduced graphene oxide (RGO), and single-walled carbon nanotubes (SWNTs) are triggered by NIR light and are used as photothermal therapy (PTT) agents. Furthermore, in order to enhance the therapeutic efficiency of light triggered therapies and at the same timeavoid the contrary side effects of the mono–therapy (PTT or PDT), the combinational use of different light-triggered therapies in a single platform was developed. Due to the rapid development of the field of material science, thanks to nanotechnology, different light triggered co-therapy modalities have been well developed by designing smart multifunctional materials such as HNCs, into which several different types of therapeutic agents together with imaging agents can be combined[130].

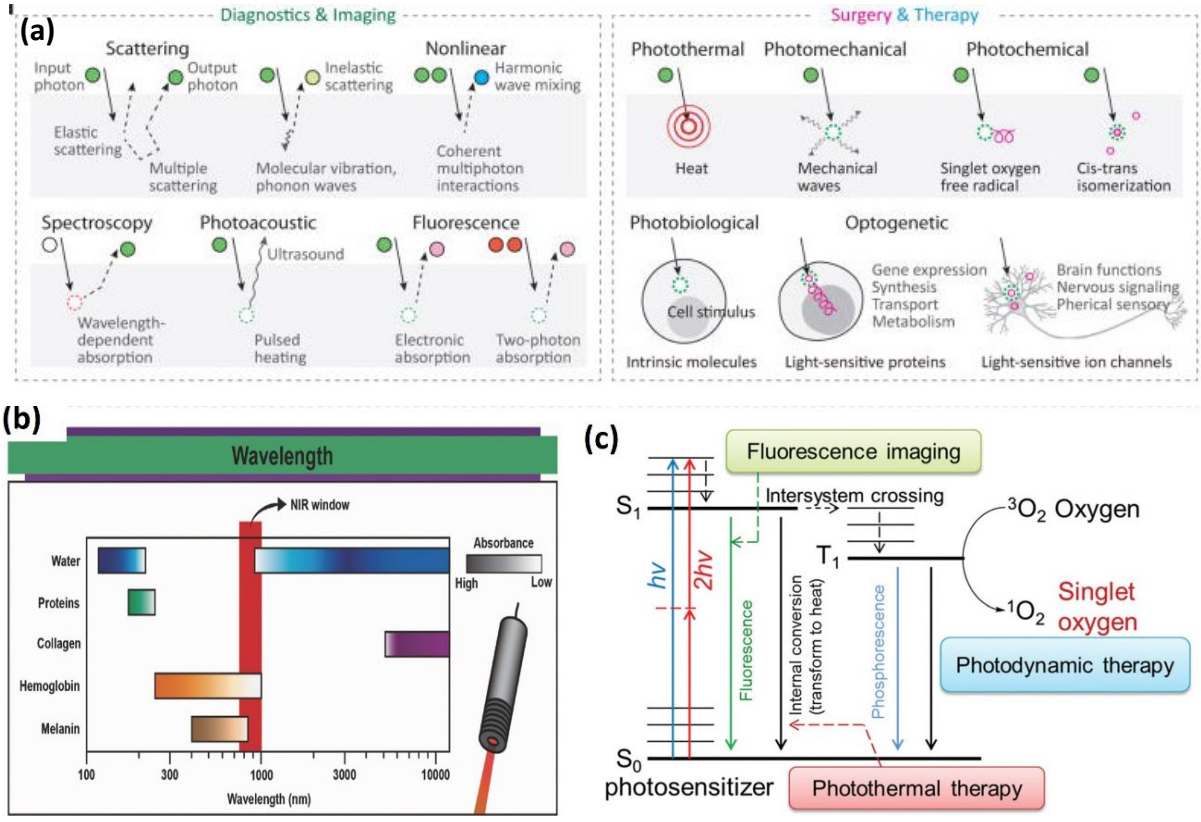

Fig. 10 Light–tissue interactions. (a) Representative optical mechanisms used in diagnosis and imaging (left), and surgery and therapy (right). Circular objects denote incoming and outgoing photons, with their trajectories indicated by solid and dotted arrows. Colours of the circles represent the spectrum of the light; dotted circles indicate the absorption of input photons. For the case of therapy, specific effects of light on tissue and cells are indicated. Reproduced with permission from Ref[128]. Copyright © 2017 Macmillan Publishers Limited, part of Springer Nature. (b) Schematic representation of the parameters related to the laser light that influence the PTT mediated by nanomaterials. In the wavelength panel, the bars represent the absorption of different bio-components and the color intensity is proportional to their absorption at that specific wavelength. Reproduced with permission from Ref[131]. Copyright© 2017 WILEY-VCH Verlag GmbH & Co. KGaA, Weinheim. (c) Energy diagram for a conventional organic photosensitizer, molecular oxygen and related photophysical and photochemical processes.

Abbreviation: hv, one-photon absorption; 2hv, two-photon absorption; S_0, ground state; S_1, singlet state; T_1, triplet state. Fluorescence, photothermal therapy, and photodynamic therapy are related to different transformation processes of the absorbed energy. Reproduced with permission from Ref[132]. Copyright© 2017 The Royal Society of Chemistry.

A. Photodynamic therapy

a. Underlying physics

Photodynamic therapy (PDT) is a physicochemical dynamic process that involves three principal components: a photosensitizer, light, and oxygen. All these components interact with each other on the same time scales relevant to a single treatment. Fundamentally, the photodynamic process depends on the photosensitizer molecule as well as the nanomaterial itself. A photosensitizer (PS) absorbs a photon of light and becomes activated from ground state (S_0) to a short-lived excited singlet state (S_1) (**Fig. 10c**). This excited state and the ground state are spectroscopic singlet states. The excited PS may either decay back to the ground state by generating fluorescence, or it can endure an intersection journey through which the spin of its excited electron reverses to form a relatively prolonged triplet state[133]. On the other hand, a high probability of transition from S_1 to an excited triplet state T_1 is possible. The triplet excited PS can then directly transfer its energy in the form of a proton or an electron to a substrate, such as the cell membrane or a molecule. This energy transfer process forms a radical anion or cation, which then reacts with oxygen to produce oxygenated products such as superoxide anion radicals ($O^{-}2$), hydroxyl radicals ($^{\cdot}OH$), or hydrogen peroxides (H2O2) (type I reaction). Alternatively, in the T_1 state, the photosensitizer can transfer energy to molecular oxygen ($^3O_2$) exciting it to its highly reactive singlet state ($^1O_2$)[134] (type II reaction). Very small amounts of energy (~22 kcal mol^{-1} correspond to wavelength of 1274 nm) are required to produce $^1O_2$ through the transition of oxygen from triplet ground state to excited singlet state[133]. The resulting derivatives of this process are type I and type II reactions that are responsible for the therapeutic PDT effect.

In cancer theranostics, PDT depends on the ability of PS to transfer energy from lasers to tumour-dissolved oxygen (O_2) to generate cytotoxic singlet oxygen ($^1O_2$), and its effectiveness is impaired by an inadequate oxygen supply in tumours[135]. Thus, a cumulative dose of singlet oxygen is an essential factor, which is presumed to be predictive of tissue damage. This prediction is quantitatively assessed using dosimetry techniques. The prediction of singlet oxygen dose on the basis of measurable quantities that contribute to the photodynamic effect such as the distributions of light, photosensitizer, and oxygen are subject

to dosimetry. Strategies, physical principles and measurement techniques of explicit, direct, and implicit dosimetry are summarised in a recent review article[134]. The other parameter influencing PDT is the wavelength of light used within the "therapeutic window". This is typically between 600–800 nm. In this wavelength range, the energy of each photon (*hυ)* is moderate (≥1.5 eV) to excite the PS but low enough to penetrate into the deep tissue and tumor. The invention of lasers, allowed the production of monochromatic light that could be easily coupled into optical fibers. Together with optical fiber light sources and theranostics NPs, next generation cancer nanotheranostics enabled PDT at desired regions (tumor) without the requirement of a straight light path and complex nanostructures that are responsive to visible light or NIR light for indirect PDT activation. Finally, the underlying physical phenomenon governing

PDT in cancer theranostics is the absorption and emission of a photon with a 'Stokes shift' in wavelength and transferring the energy into heat interacting by surrounding environment; or conversion from singlet to triplet state, resulting into generation of reactive oxygen species(ROS), accompanied by photon emission type I or type II ($^1O_2$) reactions.

b. Clinical progress

PDT is an emerging tumor therapy that relies on light as a spatially and temporally precise stimulus. Optical illumination of light sensitive drug encapsulated NPs, or PS, selectively destroying malignant cells without the side effects associated with systemic treatments such as chemotherapy[136]. At the clinical stage the success of PDT depends on the potential of PS to transfer energy from lasers to tumor-dissolved oxygen (O_2) to generate cytotoxic singlet oxygen ($^1O_2$). However, this success of PDT is impaired by an inadequate oxygen supply in tumors. Established nanotheranostic methods have attempted to optimize tumor oxygenation to ensure PDT efficacy.These approaches only affect PDT-induced oxygen depletion, whereas pre-existing hypoxia cannot be reversed, which is a big barrier to its clinical use. Therefore, developing new techniques which can reverse the tumor oxygen content during PDT have the great importance for clinical success. Pre-existing hypoxia in tumors, and oxygen consumption during PDT, can result in an insufficient oxygen supply, which in turn hampers photodynamic efficacy. The problem associated with conventional PDT has been resolved using oxygen self-enriching PDT (Oxy-PDT) by loading a photosensitizer into perfluorocarbon nanodroplets[137].In clinical studies, a single-dose intravenous injection of Oxy-PDT into tumor-bearing mice significantly inhibits tumor growth, whereas traditional PDT has no appreciable effect. On the other hand, decorating platinum on photosensitizer integrated metal organic

frameworks (MOFs), can also enhances PDT and resolves the pre-existing hypoxia in tumors[138]. Another example of using next generation nanotheranostics to deliver oxygen into a tumor uses lanthanide ion-doped mesoporous hollow upconversion NPs loaded with a chemotherapeutic drug such as doxorubicin. This can achieve endogenous intratumoralH_2O_2-responsive self-sufficiency of O_2 and NIR light controlled PDT simultaneously for overcoming hypoxia cancer[139].

In addition to those technologies that focus on replenishing hypoxia in tumors, new paradigms can generate singlet oxygen ($^1O_2$) under NIR photoirradiation along with chemotherapeutic action in hypoxic tumor microenvironment to diminish O_2 dependence.. The clinical proof-of-concept has been validated by developing a semiconducting polymer nanoprodrug (SPNpd)[140]. The well-defined and compact hybrid SPNpd (30 nm) is assembled from amphiphilic polymer brush, which comprises a light-responsive photodynamic backbone grafted with poly(ethylene glycol), and conjugated with a chemodrug through hypoxia-cleavable linkers.. Cancer cells in hypoxic tumors are often remarkably resistant to PDT and thus next generation PDT nanotheranostics line of action is required. This has been addressed recently, by the development of a nanocomposite that contains Pt(IV) and chlorin e6, in which upconversion NPs are loaded to convert 980 nm near-infrared light into 365 nm and 660 nm emissions[141]. In clinical experiments this nanocomposite accumulated at the tumor site. A 980 nm laser was used to trigger the nanocomposite to generate O_2 for consumption in the PDT process and releases active Pt(II) for synergistic photo-chemo therapy to enhance PDT antitumor efficiency. Earlier work published in 2018[142], reports type II PDT to overcome the tumor hypoxia barrier. Type II PDT is a form of phototherapy involving light and a photosensitizer. Researchers successfully fabricated O_2-generating HSA-MnO_2-Ce6 NPs for enhanced photodynamic effect by conjugating molecular oxygen (O_2) to produce singlet oxygen ($^1O_2$). This approach leads to cellular necrosis and apoptosis in bladder cancer by overcoming hypoxia. As a minimal or noninvasive nanotheranostics approach for tumors, PDT induced by external laser irradiation coupled with various nanosystems has been used to treat various type of cancers at the clinical stage, including; nano-liposomes[143], magnetofluorescent carbon dots[144] and biomimetic MnO_2@PtCo nanoflowers[145] (hypoxia breast tumor), phosphorus nanosheet[146] (HeLa tumor), calcium carbonate-polydopamine nanocomposite[147] (skin tumor), 5-fluorouracil (5- FU)-loaded silk fibroin NPs[148] (gastric tumor), supramolecular silicon-containing nano dots nanogel[149] (lung cancer), CRET-based biomimetic silica nanoreactor[150] (lung metastasis tumor), and many others which are reviewed in recent review articles[151,152].

c. Next generation PDT device design

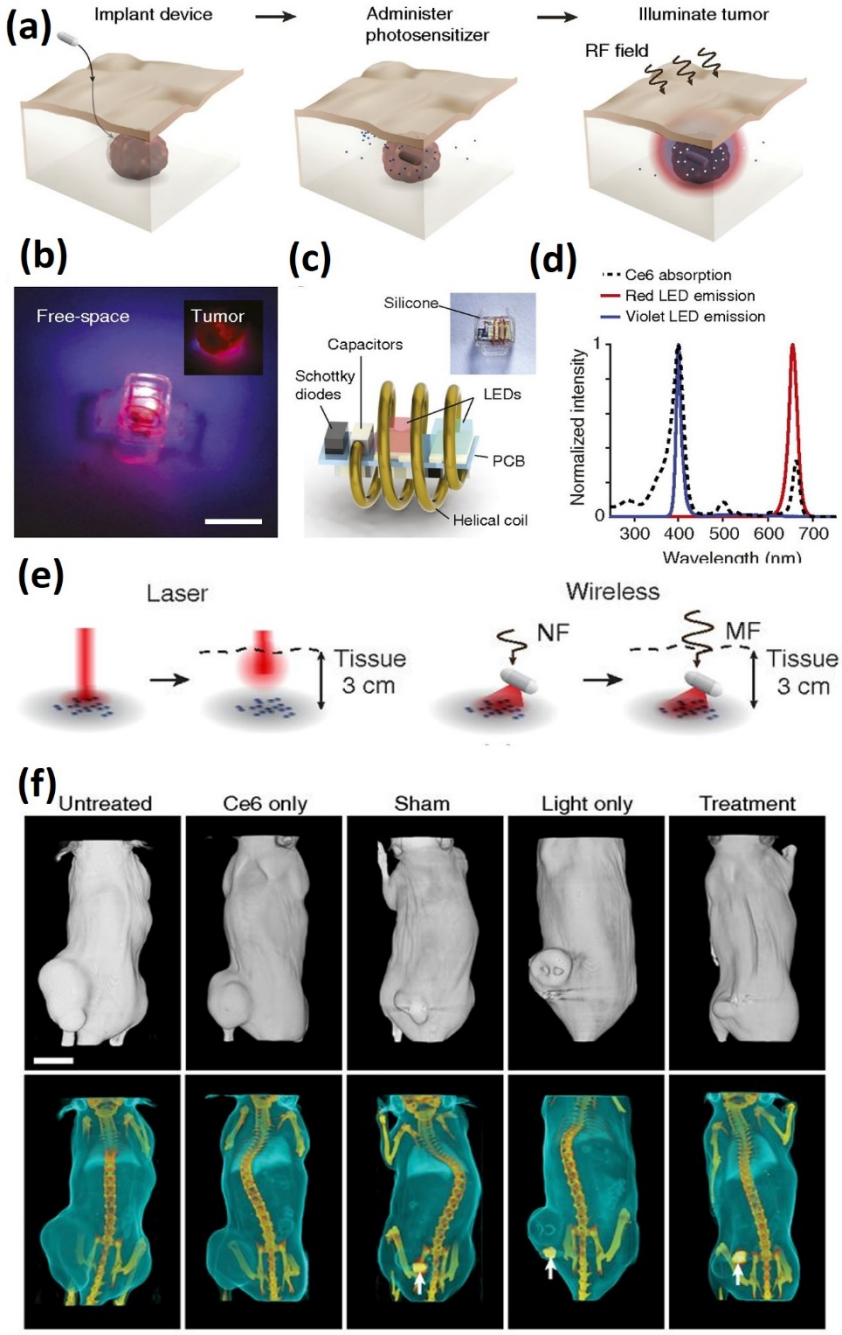

Fig. 11 Next generation wireless photonic PDT device. (a) Schematic of the PDT therapy. The therapy consists of implantation of a wireless LED near the target region, administration of the photosensitizer, and wireless powering of the device. Light emitted by the device locally activates the photosensitizers and induces tumor damage. (b) Image of the wireless photonic device emitting light. (Inset) The device illuminating an explanted tumor. (Scale bar, 2 mm.) (c) Schematic of the device and individual electronic components. (d) Optical emission spectrum of the device from two LEDs. The emission wavelengths are centered at 400 nm (violet) and 660 nm (red), overlapping with the absorption peaks in the Ce6 spectrum. (e) Illustration of light-delivery configuration for irradiating MB49 cells using laser and device, with and without intervening thick porcine tissue. Near-field (NF) wireless powering is used at close proximity and midfield (MF) for thick tissue (f) In vivo PDT, CT reconstructions of representative mice in each group 13 d after first treatment. White

arrows show implant position. (Scale bar, 1 cm.). Reproduced with permission from Ref[153]. Copyright© 2018 PNAS license.

The low penetration depth to less than a centimeter of light within tissues currently limits the therapeutic efficiency of PDT even at NIR wavelengths. Presently, optical fibers inserted through surgery or endoscopy are used to deliver light into deeper tissue regions. However, this approach allows only a single light dose to be delivered and is incompatible for long-term implantation. To deal with this issue, scientists from the National University of Singapore developed a nanotheranostic approach based on a wireless photonic device that enables on-demand light activation of photosensitizers deep in the body for targeted PDT[153]. The biomedical engineering approach used to treat tumors, allowing deep operation near organs at human size scales, multi- wavelength light emission at radiant power levels for nano photosensitizer activation, and wireless control of light emission for therapeutic dosimetry (Fig.11). The wireless delivery of light deep in the body *in situ* by activating photosensitizers can potentially provide advantages in the clinic to treat hepatocellular carcinomas or brain tumors. On the contrary, Yuji Morimoto and colleagues made-up a wireless PDT system for metronomic cancer treatment (low-dose and long-term PDT) that uses stretchable poly(dimethylsiloxane) (PDMS) nanosheets modified with mussel-footprotein-derived bioadhesive polydopamine (PDA)[154]. Ultrathin PDMS nanosheets fabricated by a roll-to-roll process, and decorated with PDA, can form strong chemical bonds with biological tissue surfaces[155]. The designed nanodevice is showing strong antitumor effects and could be an alternative to current therapies used to treat localized tumors, favoring the clinical applicability of the PDT in fragile or delicate organs system.. Researchers in Fudan university fabricated a NIR rechargeable “optical battery” for irradiation-free PDT. The nano-device embeds upconversion materials, persistent luminescence materials, and a photosensitizer into biocompatible polydimethylsiloxane[156]. The optical battery can be continuously charged using 980-nm NIR laser within very short time (~5s) to generate singlet oxygen in deep tissue (~4 mm) under green persistent luminescence with low photothermal effect. The effective deep tumor proliferation inhibiting capability of this NIR rechargeable “optical battery” may give rise to the next generation of intelligent stimuli-responsive nanotheranostics in the clinic. Endo-laparoscopy based on endoscopic equipment, is a technique used in the treatment of gastrointestinal cancer, which could also be used to deliver light to tumor sites. The combination of endoscopic light guidance with NPs based photosensitizers makes it possible to treat cancer via PDTwhich would be difficult to treat with endo-laparoscopy surgery or PDT.

Kim*et.al*., designed a polymeric nanoassembly conjugating tumor targeting aptamers to perform effective endo-laparoscopic PDT[157]. Under laser light irradiation, the nanoassembly not only showed improved in tissue penetration, but also induced the death of tumor cells through apoptosis, signifying great potential to be translated into clinics for endoscopic tumor diagnosis and treatment.

B. Photothermal therapy

a. Underlying physics

Photothermal therapy (PTT) relies on the photothermal effect of photothermal transduction agents (PTAs) that can harvest the energy from light and convert the energy into heat. The heat generated (42.5–43.0 °C) can be further utilized to trigger the death of tumor cells by photo-hyperthermia. Metallic NPs are efficient PTAs that convert electromagnetic radiation into heat *via* plasmonic resonances[158]. This feature has been displayed by several types of metallic nanostructures produced with gold, carbon, copper, molybdenum, tungsten, iron, palladium or novel new generation HNCs. Different strategies to improve NP mediated cancer PTT have been highlighted in a recent review article[131]. NPs optical response is a function of scattering (σ_{Scat}) and absorption cross sections (σ_{Abs}). The heating power (P) of a metallic NP under continuous light exposure is proportional to the incident light intensity (I) and the absorption cross section: $P = I \times \sigma_{Abs}$.. The absorption cross section of metal NPs is influenced by the size, shape and elements of NPs. When nanostructures are irradiated with light, the excited electrons rapidly accumulate on their surface, which is known as localized surface plasma resonance (LSPR) effect. Electronic oscillation in the nanostructures will dampen *via* transferring energy to the environment in the form of heat. The penetration of light into deep tissues is limited due to the attenuation of human tissue. This could be resolved by utilizing light sources at wavelengths where the human body is most transparent (biological transparency windows (**Fig. 10b**)). So far, PTAs are built to respond to the NIR-I (700-950 nm) & NIR-II (1000- 1350 nm) region in clinically demonstrated PTT. Very recently, advancing optics and biomedical engineering developed novel photodetectors technology that gave new transparency windows at longer wavelengths: NIR-III (1600-1870 nm) and NIR-IV (2100-2300 nm) for PTT[158]. Utilizing NIR-III & IV assures better light penetration into deep tissue with less attenuation. Alternatives to overcome the light penetration issue, are to use fiber optics to transmit light through human body into tumors, and activate PTAs for effective PTT outcome. Acting as a stand-alone conventional laser based PTT, NP mediated PTT

provides efficient light-to-heat conversion and the ability to penetrates tissue more deeply than of light by tuned absorption of NIR light.

b. Classification of nano PTAs

The past few decades have witnessed rapid developments in nanotechnology towards developing novel NPs and ‘‘smart’’ PTAs for PTT. Ideally, PTAs transform energy from absorbed light into heat and increase the temperature of the solid tumor. PTAs are usually categorized into inorganic and organic materials. Inorganic PTAs contain noble metals, graphene and carbon nanotubes, boron nitride NPs. Organic PTAs include NIR-responsive small molecules and semiconducting polymer NPs[159]. Among the inorganic NPs, gold-based nanostructures like gold NPs (AuNPs), nanorods (GNRs), nanocages, nanohexapods, nanoshells, and nanostars, have been intensely investigated for PTT. An important feature of Au NPs is that their size range can be easily varied to yield maximal absorption within the first NIR window (650–850 nm), which can safely penetrate 2–3 cm of tissue. Different from AuNPs, GNRs have a short and long axis, thereby showing two absorption peaks corresponding to the transverse ($\lambda \approx$ 500–550 nm) and longitudinal ($\lambda \approx$ 650–850 nm) surface plasmon resonance (SPR)[160]. The latter strongly depends on the nanorod shape and can be adjusted to the NIR region by increasing the ratio aspect of nanorods. Using the novel synthesis ways, GNR dimensions can be shortened or elongated to achieve peak longitudinal SPR in the NIR region. GNRs with dimension 10 nm × 40 nm, for example, can maximally absorb ~800 nm light and are therefore the most common for PTT. At present, many other inorganic carbon based nanostructures such as carbon nanotubes (CNT) and nanographene oxide (nGO) are being actively studied for tumor PTT. The other inorganic nanostructures studied for PTT at the preclinical stage are copper (Cu) based copper sulfides (e.g. $Cu_{2-x}S$ nanodots, $Cu_{7.2}S_4$ nanocrystals) , molybdenum (Mo), tungsten (W), iron (Fe), palladium (Pd) based NPs, Mo and W- based oxides (e.g.MoO_{3-x} hollow nanospheres, WO_3 nanoparticles) and disulfides (MoS_2 and WS_2 nanosheets), Pd nanosheets etc[161]. On the other hand, only a few organic nanostructures such as polyaniline (PANI), polypyrrole (PPy), poly(3,4-ethylenedioxythiophene) (PEDOT) plasmonic nanoliposomes are found to be effective in PTT[162]. Even though PTT of tumors in small animals has been reported over the last decade using the NPs mentioned above, , clinical translation has been extremely slow, as very few of these NPs are now under clinical trials[163]. Many comprehensive reviews, addressing synthesis processes, physical chemical properties of NPs, and their relevance to PTT have already been published[159–161,164]. Among them, plasmonic GNRs have reached the clinical stage because of

their strong photon energy absorption cross section and ability to transduce light into heat with high efficiency. However, the state- of- the- art of clinical research stage and new generation nanotheranostics PTT devices are not being reviewed yet. Thus we are focusing on the most up-to-date PTT devices advancing the nanotheranostic and clinical stage reports, in the following section.

c. Clinical progress

PTT combined with nanotechnology has become a powerful tool to treat cancer. Despite the tremendous development in PTT coupled with different NPs, there are still major obstacles to clinical translation such as batch-to-batch variation, lack of verification of therapeutic efficacy in tumor site, difficulty of site-selective thermal dosing, and relatively limited size of ablation zones. To address these core issues, an HNC based "smart" nanotheranostic approach has been proposed by Liu and coworkers[165]. This smart nanoplatform consists of a core of magnetic gold nanowreaths, which provides excellent photothermal property, and a shell made from the self-assembly of exceedingly small magnetic IONPs. The novel HNCs not only enhanced their tumor accumulation by inhibiting their fast-renal clearance, but also generated glutathione (GSH)-responsive MRI T_1 signal in the tumor micro-environment. In addition to the bright T_1 imaging, HNCs were also able to greatly enhance the photoacoustic imaging contrast in the tumor, which further helped to determine the site-selective PTT dosing and best time point to conduct PTT.. In another recent study, unique rabies virus-mimetic silica coated GNRs were used to overcome the blood brain barrier (BBB) and treat brain tumors using PTT[166]. Importantly, it is of great interest that these nanorods not only resembled the appearance of the live rabies virus but targeted the brain through the neuronal pathway bypassing the BBB. Also, smart HNCs were able to induce a photothermal effect in response to NIR laser (808 nm) irradiation, based on localized SPR, to effectively suppress brain tumors during clinical experiments using a nanotheranostics platform.

The scattering and absorption of light in biological tissue strongly impedes the penetration of laser light. Thus, it is difficult to determine the distribution of light into an organ to evaluate the temperature distribution at different depths of a tumor tissues. In aconventional PTT approach, tumor cells were injected subcutaneously, NPs were administered systemically or locally, and laser light was typically applied to the skin at an intensity of higher than the threshold limit (~420 mW/cm^2) for the induction of PTT. This approach inducesskin damage due to thermal injury, and hence, a new nanotheranostic practice that utilizes NIR laser light and NPs without inducing skin damage is required. Sugiura and his group from the Tohoku

University, Japan have designed a new NPs based PTT protocol involving computational simulations for the treatment of aggressive metastatic tumor using NIR laser light, GNRs, and a skin temperature control system[167]. The temperature distribution and region of the tumor showing damage were determined by numerical analysis after considering the degree of light scattering. Using this new light based cancer nanotheranostic concept researchers were able to eliminate cancer tumor under NIR irradiation and advance effective anticancer therapy that did not induce macroscopic skin damage. The adequacy of cancer PTT involves a balance between eradicating the entire lesion for cancer clearance but without compromising much of the healthy surrounding tissues. Clear tumor boundaries are essential for this curative approach. A novel endoscopic approach integrated with multifunctional GNRs was used by Singh et.al. in 2019, as a non-conventional nanotheranostic approach to treat upper gastrointestinal cancer[168]. GNRs were functionalized with an optical fluorophore (Cy5.5) modified with anti-EGFR antibody, together with image-guided NIR irradiation, to enhance cancer site-specific fluorescence and PTT. Clinically relevant intravenous GNRs administration route is taken to overcome the molecular heterogeneity within tumors and endoscopic intravenous injection followed by PTT has induced gastrointestinal tumor debulking. When assessing clinical suitability, nanotheranostics coupled PTT should fulfill the criteria of (i) deep tissue penetration of NIR light, (ii) resistance to photobleaching, (iii) enzyme degradation, and (iv) high extinction coefficients for effective light absorption. The nanotheranostics way offered by Singh *et al*., are fulfilling all these benchmarks as GNRs are resistant to photobleaching, enzymatic degradation, and have a 4-6 orders higher extinction coefficient which permits more effective light absorption than common photosensitizers.

Local ablation, for example PTT are increasingly employed for treating nonresectable solid tumors in the liver, this has been clinically validated on 14,150 colorectal liver metastases (CRLM) patients, strong survival benefit with a 26.9% and 5 year overall survival achieved for those undergoing local ablative liver-directed therapies[169]. Although these local ablative PTT have found great potential, they are also limited by the size and location of tumors and off-target effects such as bile duct or vascular injury due to the percutaneous insertion and nonspecific heating by ablative probes. Recently, Parachur *et al*., from the Medical College of Wisconsin, United States, developed a PTT device for tumor-selective interventional radiology-guided liver cancer therapy [170]. The primary purpose of this innovation was to demonstrate a proof-of concept for an efficient hepatic site-selective delivery of trimodal optical/MR/X-ray contrast-bearing GNR-based theranostic NPs (TNPs) by a minor modification of the existing interventional image-guided clinical procedures (**Fig. 12**). Site-

selective delivery of TNPs is achieved *via* the hepatic portal vein and PTT using a catheter based 808 nm NIR laser. TNPs with a GNR core and inorganic Gd(III) layer that retain shape and ablative capability over multiple cycles and are stable *in vivo*, while providing usable MR and CT contrasts on clinical scanners for clearly visualizing CRLM tumors.

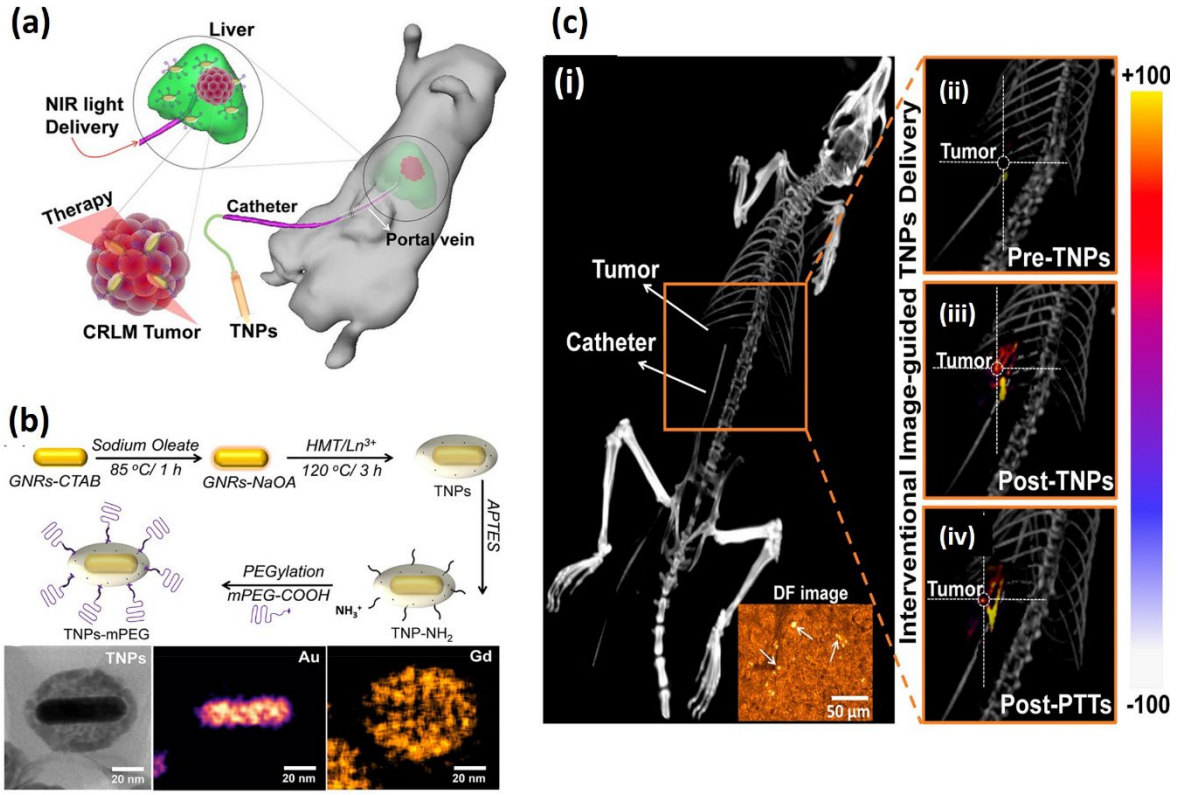

Fig. 12 (a) Schematic illustrating the site-selective delivery of TNPs via the hepatic portal vein and PTT using a catheter-based 808 nm NIR laser. (b) Schematic for the synthesis of TNPs along with STEM image demonstrating the morphology of TNPs and Au/Gd elemental mapping. (c) Interventional image-guided TNP delivery and therapy. (i) 3D reconstructions of Dyna CT image of a rat with a CRLM tumor, where the catheter was placed in the liver via a portal vein. Rats were injected with TNPs followed by saline. DynaCT image of rats (ii) pre-TNPs, (iii) post-TNPs, and (iv) post-PTT. Inset of (i) shows the dark-field image of CRLM tumor tissue having TNPs; pointed arrows indicate scattering from TNPs. Reproduced with permission from Ref[170]. Copyright © 2018 American Chemical Society.

The combination of "chemotherapy + PTT + imaging modalities" with different organic therapeutic agents and anticancer drugs may supportively suppress tumor progression by utilizing the advantages of both modalities and circumventing the drawbacks of each modality. Novel organic HNCs could be self-assembled into nanodrug self-delivery systems for combinational cancer nanotheranostics. An active stealth nanotheranostic strategy was explored by Li.et al., by applying small molecular photothermal agent and chemotherapeutic drug to construct carrier-free nanomedicines for multimodal imaging-guided PTT[171]. Indocyanine green (ICG) and epirubicin (EPI) are co-self-assembled into small molecular nanoassembly. Nanoassembly promoted photothermal response, excellent NIRF/PA imaging

properties, pH-/photo-responsive drug release behavior, and cellular endocytosis. Furthermore, multifunctionality of this nanotheranostic system provided real-time self-monitoring intracellular drug delivery and image-guided synergistic combination therapy in clinical stage. Several other organic nanoassemblies have been proposed in attempts to enhance combinational chemo-PTT outcomes in preclinical stage; such as nano-colloidosomes loaded with DOX/ICG[172], methotrexate-hyaluronic acid–octadecylamine-curcumin nanoassembly[173]. In contrast to inorganic NPs, NIR responsive organic NPs bypass the issue of metal-ion induced toxicity and thus are generally considered to be more biocompatible. Inorganic NPs possesses size-dependent SPR properties, organic NPs have size-independent optical properties, making it feasible to develop NPs with the ability of multimodality at different wavelengths with similar biochemical properties. We encourage readers to go through recent review article, where all optical, chemical, physical properties of various organic NPs are introduced, further followed by the discussion of the PTT and PDT systems[174]. Despite a tremendous amount of exciting different type of NPs and their preclinical results reported in the past few years, however, the further clinic application of PTT is still difficult. The successful combinations of NPs-PTT (NPTT) adjuvant therapy approach and surgery can certify the great potential in clinical operations in post-surgery or pre-surgery with prominent features. In the early 2019 this concept has been validated similar to that of neoadjuvant chemotherapy; therefore it termed as "neoadjuvant NPTT"[175]. Preoperative neoadjuvant NPTT could supress the breast tumor in a short time and make the boundary between the tumor tissue and surrounding healthy tissues clearer, therefore, creating conditions for better surgical resection. However, this novel light therapy is more suitable only for some types of superficial tumors at present, owing to the limited light penetration depth of the NIR laser.

d. Next generation device design

The next -generation light activated cancer nanotheranostic strategies seek to maximize the penetration of light, permeability of the drug to the tumor and therapy using HNCs coupled with biomedical devices without damaging the healthy environment outside the tumor region. Catheter-based light guiding systems can transmit the light direct to tissue in this fashion that only diseased tissue can exposed to light. The novel technology includes a first type of catheter configured for photo-activating photosensitive materials in tumor and a second type of catheter configured for photo-degrading photosensitive materials in tissue[176]. Likewise, electrospun nanofiber device is designed to induce efficient and repeatable PTT when exposed to 808 nm NIR light without loss of heating capacity[177]. When implanted at the tumor site, this

nanodevices is making contact with the tumor directly, thus enabling continuous localized PTT and drug release under continuous light exposure.

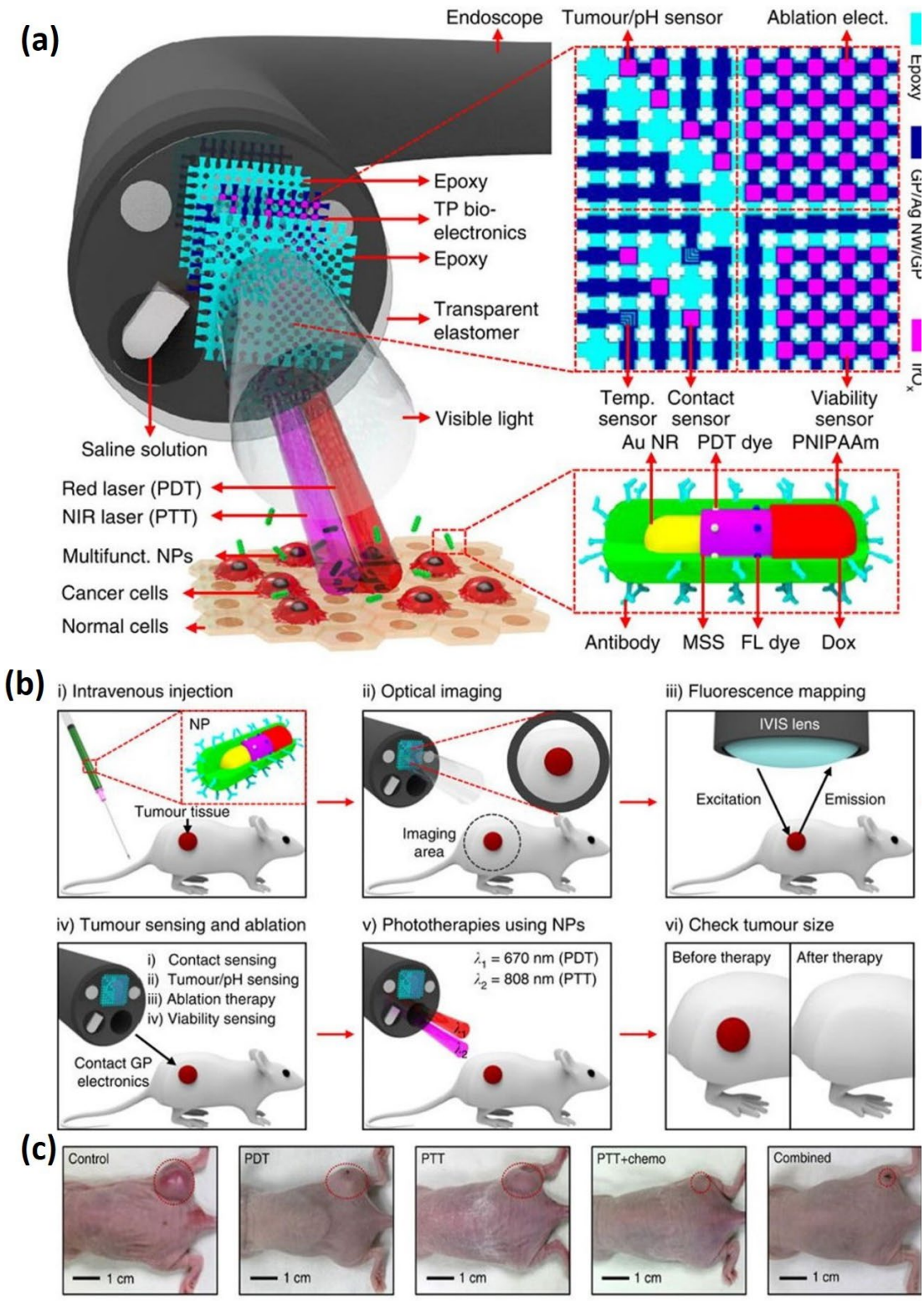

Fig. 13 A multifunctional endoscope system. (a) Schematic illustrations of the design strategy and mode of use for the multifunctional endoscope system based on transparent bioelectronic devices and theranostic nanoparticles. (b) Schematic illustrations of tumor treatment procedures with the multifunctional endoscope.

(c) Images of the mouse model with HT-29 tumors after multimodal treatments (from left to right: control, PDT, PTT, PTT + chemo and combined therapy). Reproduced from ref[178]. Copyright© 2015 Nature Publishing.

Advances in optics and fiber optical technology resulted into new generation endoscopes, that offering both diagnostic and therapeutic capabilities including tissue biopsy and resection of tumors. The new generation endoscopes not only providing alternatives to surgical resection but also guiding intraprocedural mapping of cancerous tissues, controlling the delivery of NPs for theranostics. Thus, it is possible to obtain precise information about the location and physicochemical properties of the targeted growth of tumor or diseased organ. Researchers from Institute for Basic Science (IBS), Seoul, Republic of Korea demonstrated the 'smart' surgical endoscope system as novel nanotheranostic approach to diagnose and treat colon cancers[178]. This endoscope is configured with transparent bioelectronics, which provides impedance- and pH-based sensing, in combination with radiofrequency (RF) ablation therapy to facilitate the characterization and removal of colon cancers (**Fig. 13a**). In addition to bioelectronics, this system has custom-designed biocompatible theranostic NPs with PTT, PDT and chemotherapeutic agents, which can be delivered locally and activated with light. The endoscope allows laser light to access suspicious sites exposed to NPs. PDT, PTT and chemotherapies induced by nanoassembly containing PDT dyes (chlorin e6; Ce6), GNRs, Dox, loaded in the mesoporous silica shell, this can effectively destroy any residual cancer cells around the surgically treated area on activation with irradiated NIR lasers (**Fig 13b, c**). This smart endoscope facilitate access to internal tumors and provide a significant amount of diagnostic feedback during treatment routines, thus highlighting the utility of this technology in the translational medicine. Kress and colleagues from the Wright State University, Dayton, USA, have demonstrated light based dual-channel endoscopic technique for quantitative reflectance and fluorescence imaging for monitoring of local drug concentrations in target areas such as tumors[179]. Importantly, the endoscope serves for light delivery to trigger in vivo drug release in ovarian cancer. This technology demonstrates the localized NIR-light triggering of chemotherapeutic drug from nanoliposomes with minimally invasive, quantitative measures *in vivo* for fast clinical translation.

C. Two-Photon light therapy

a. Underlying physics

At present, one of the main challenge for light activated cancer nanotheranostics is, how to improve the delivery of low-energy photons of visible/NIR light into deep-seated tumors. Nanomaterials that absorb light in the phototherapeutic window in a multiphoton fashion have several advantages for light triggered therapy and imaging. Multiphoton absorption causes the materials excitation by two or more photons, where a single photon is not sufficiently energetic, this novel approach is termed as two-photon absorption (TPA). Moreover, TPA nanomaterials normally have large two-photon absorption cross-sections, which hold great potential as efficient two-photon donors in light activated nanotheranostics. The advantages to such an unconventional theranostics approach include (i) higher in-depth light penetration in tissue since materials are repeatedly triggered by red or near-infrared (NIR) light and (ii) the prospective to selectively stimulate the material in a physiological medium[180]. In particular, NIR two-photon sensitive nanodevices benefit the three-dimensional resolution and the low scattering losses of the irradiation in biological tissues, and thus safer and more selective treatments.

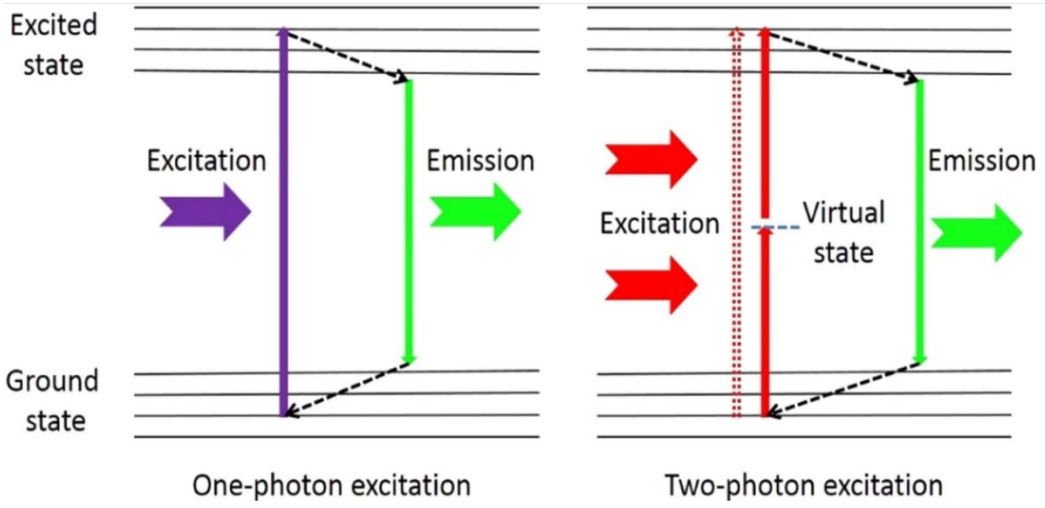

Fig. 14 Energy diagrams showing one-photon absorption (OPA), two-photon absorption (TPA). Reproduced with permission from Ref[181]. Copyright© 2017 IOP Publishing Ltd.

TPA-induced excitation of HNCs (photosensitizers) is a more promising approach to increase the penetration of light into tissue. The development of TPA HNCs can be achieved by the conjugation of dye molecules onto the nanostructure. The dye molecules simultaneously absorb two photons of lower energy to an excited electronic state (**Fig. 14**); these excited molecules react with oxygen to generate singlet oxygen which can be used to induce cell death.

When two-photon dyes are excited in the NIR, light can penetrate deeper into tissue as between 800 nm and 1400 nm, there is minimal absorption and scattering of light. Indeed, TPA light theranostics combines PDT, PTT and tissue fluorescence imaging on the principle of simultaneously absorption of two photons with the same energy to the excited singlet state pass *via* a virtual intermediary state. New class of HNCs integrates the advantages of two-photon excitation (TPE) with those of nanotechnology as novel photosensitizers (PSs). HNCs explores basic physical mechanism of PSs via absorbing two lower energy photons of infrared light and the sum of the photon energies are equal to the band-gap of energy. However, one-photon excitation of PSs requires the absorption of a single photon equal to the band-gap energy of the PSs. Thus, this novel nanotechnology coupled TPA thereby allowing for deeper light penetration and lower photo-bleaching of PS molecules in tissues[182]. The TPA is a nonlinear photon absorption process, thus it makes possible to activate PSs at the focal point of the laser light, further allows for better spatial control of PSs activation in three-dimensions in therapy and imaging, reducing off-target destruction to surrounding noncancerous tissues during PDT or PTT.

b. Clinical progress

Two-photon excitation is extending the functional window of NPs by nonlinear excitation mechanism in the NIR region. In the course of in vivo experiments, TPE is reducing the photobleaching of NPs and providing a higher spatial image resolution in contrast to one-photon excitation[183]. The next generation TPE nanodevices are combining diagnosis and image-guided tumor therapy using a single hybrid PSs and advancing clinical potential of cancer nano-phototheranostics. In the year 2006 Gao and co-workers, proposed use of NPs as TPE PSs to treat brain cancer by PDT[184]. In this first investigation on such hybrid nanoplatform (according to researcher's claim), the encapsulation of polyacrylamide based NPs with dye molecule TMPyP (5,10,15,20-tetrakis(1-methyl 4-pyridinio) porphyrin tetra(ptoluenesulfonate)) is performed to evaluate their anticancer efficacy with and without PDT for rat C_6 glioma cells. NIR light excitation of this HNCs allowed deeper tissue imaging and enabled deeper tissue two photon PDT while killing glioma cancer cells in vitro. Meanwhile in the year 2007, Durr and co-workers demonstrated the use of GNRs as bright contrast agents for two-photon luminescence (TPL) imaging of cancer cells in a 3D tissue phantom down to 75 μm deep[185]. At 760 nm excitation light, hybrid GNRs have improved tumor cells imaging brightness by 3 orders of magnitude compared with two-photon auto fluorescence emission intensity from unlabelled cancer cells.

Fortunately, tremendous progress in the present decade on different type of HNCs design and development in optical technology provides an unconventional way to realize TPE in cancer nanotheranostics by implementing NIR-to-visible conversion pathway in the tumor. For instance, hybrid gold nanocages with lipid-hypocrellin B are designed for the TPE combined treatment of PDT and PTT for ablation of tumor cells in vitro[186]. This two-photon activated nanoassembly (photosensitizer and photothermal transducer) has minimized the PSs' negative effect in the unnecessary non-targeted areas and resulted into results in one-off administration and irradiation for antitumor treatment. Primary in vitro results unlocked new clinical feature for integration of different approaches to facilitate the combined treatment. Owing to their collective outstanding properties such as good biocompatibility, high surface area, large pore volume for drug storage, broad light absorption and excellent optical properties for imaging, carbon dots are widely used as PSs, recently. For example, hallow fluorescent porous carbon dots loaded with chemotherapeutic drug can also effectively absorb and convert the NIR light to heat for regulated drug release and PTT[187]. This functional carbon HNCs can excited in the higher wavelength region with emission in the lower wavelength region and acting as optical imaging contrast agent in laser confocal and two-photon fluorescence cell imaging covering a broad excitation wavelength range from ultraviolet (UV) light to NIR light. In the year 2018, Lan and co-workers designed functional carbon dots with a high fluorescence quantum yield of 49% for integrated platform of photoacoustic imaging, NIR triggered two photon phototheranostic agent for fluorescence imaging and PTT/PDT synergistic breast cancer therapy at clinical stage[188]. Several recent studies reports various functional carbon dots for two photon triggered cancer theranostics for many type of cancers at clinical stage[189–191]. In order to reduce tumor hypoxia and meet the clinical demands, two-photon light controlled nano-PSs are developed; including Ru (II) complex loaded Fe-C_3N_4 nanocomposite[192], Bis(pyrene)-Doped Cationic Dipeptide NPs[193], Dendrimeric NPs[194], hybrid $NaGdF_4$:Yb,Er@$NaGdF_4$:Nd,Yb UCNPs[195] etc. Most nano-phototheranostics modalities proposed before, involve PDT/PTT and NPs that have low photosensitizing efficiencies, tumor resistance, and lack of spatial resolution. On the contrary, new generation engineered two-photon-sensitive organosilica HNCs showing higher photosensitizing yields, versatile therapies, and a unique spatial resolution. These novel HNCs are effective at clinical stage in the treatment of retinoblastoma, breast, and skin cancers[196].

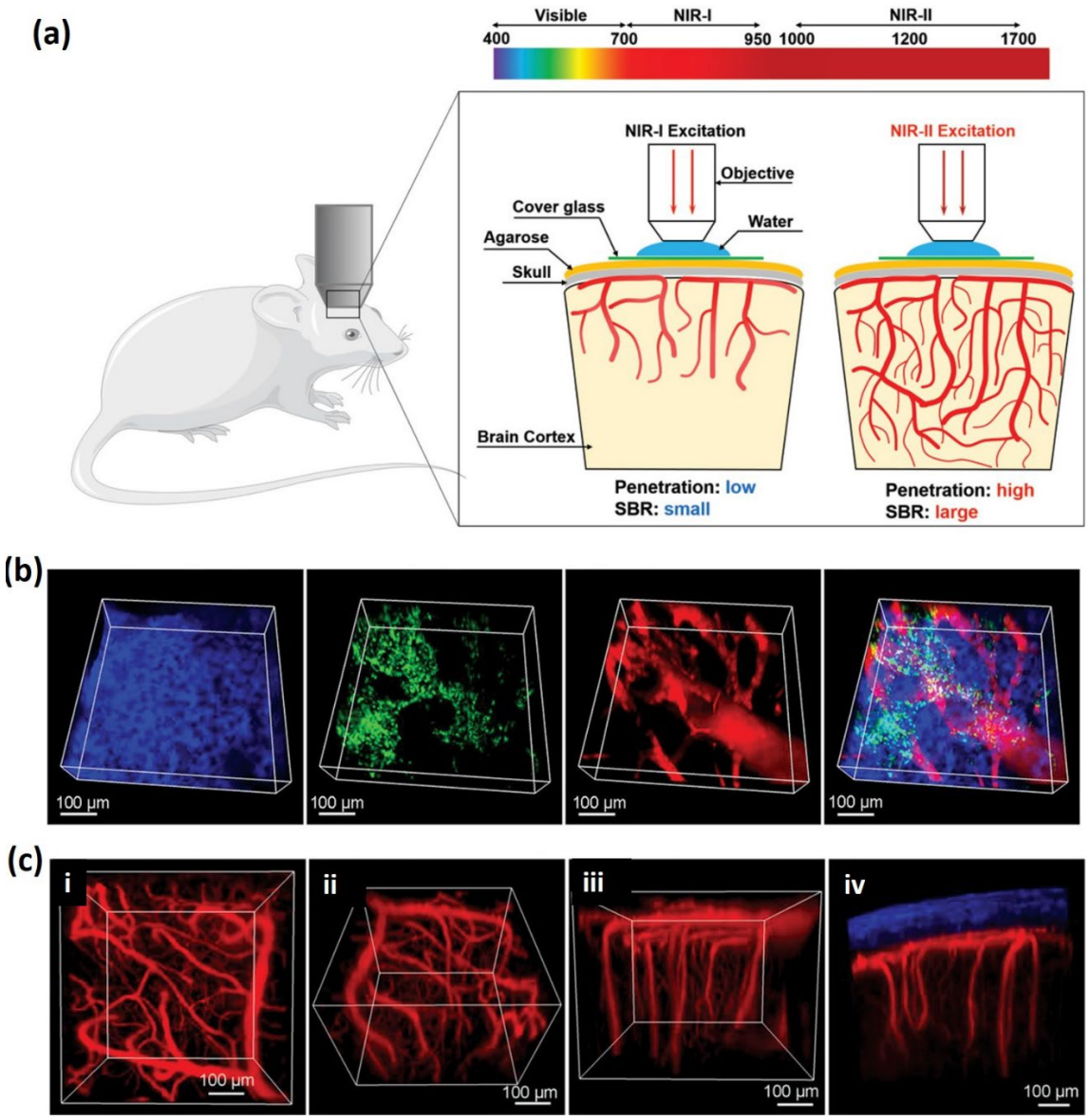

Fig. 15 (a) Schematic illustration of on NIR-I and NIR-II excited in vivo two photon excited fluorescence imaging of mouse brain. (b) 3D reconstructed in vivo two photon excited fluorescence images of bone, neutrophils and conjugated polymer dots and their overlay in the bone marrow. (c) 3D reconstructed photon excited fluorescence images of the brain blood vessels. (i-iv) 3D reconstructed image showing the position of the skull and the brain blood vessels network below the skull. Excitation for SHG: 950 nm; Excitation for 2PF: 1200 nm. Emissions were collected within 455–500 nm for SHG, and 660–750 nm for conjugated polymer dots. Each frame was acquired in 3.22 s. Reproduced with permission from Ref[197]. Copyright©2019 WILEY-VCH Verlag GmbH & Co. KGaA, Weinheim.

The growing demand for observation and understanding the structures and activities of central nervous system (CNS) and CNS brain tumors, noninvasive brain imaging are highly desirable. Two-photon activated HNCs with NIR light excitation is novel and relatively noninvasive approach, recently proposed to study brain with high spatial resolution and large imaging depth. However, clinical challenges such as cranial window implantation or skull-thinning methods, attenuation of excitation light and strong light scattering induced by skull

bone are limiting the use of light triggered nanotheranostic approach in brain cancer. To resolve these issues Alfu and co-workers designed HNCs that are conjugating organic dye 2-(4-bromophenyl)-3-(4-(4-(diphenylamino)styryl)phenyl) fumaronitrile (TPABDFN) and poly(styrene-co-maleic anhydride) (PSMA)[198]. This HNCs have presenting large two-photon absorption cross-section (5.56×10^5 GM), and bright NIR emission. Due to the deep penetration capability of both 1040 nm-excitation and NIR emission light, a very large imaging depth of 1200 μm, this HNCs have provided an effective platform for brain cancer diagnosis. Wang and co-workers in the early 2019 developed ultrasmall single-chain conjugated polymer dots (CP dots) that are showing bright NIR-I emission for NIR-II excited deep in vivo two-photon intact brain imaging[197]. In the clinical stage these light activated nanoassembly visualized both blood vessels in the skull bone marrow and brain blood vessels through skull. Furthermore, 3D reconstruction of the brain blood vessel network with a vertical depth of 400 μm was obtained through intact skull by using of bright NIR-I emission and NIR-II photoacoustic imaging (**Fig. 15**). This next generation nanotheranostics establishes the advantage of two photon excitation in NIR-II and NIR-I fluorescence emission for deep and high contrast imaging, which provides new opportunities for noninvasive imaging of brain structures and activities in neurosciences and neuro-oncology.

D. Future opportunities and challenges

Light activated cancer nanotheranostics is definitely a promising new generation treatment modality. Recent advances in biomedical optics technologies have enabled novel ways of implementing PDT, PTT and TPA in targeted cancer therapies. In particular, these modalities are integrating photonics with nanotechnology, biomaterials and bioengineering. The heterogeneity of cancerous tumors varies patient to patients, this disease diversity challenges the chemotherapeutic treatment responses. In recent years' evident based precision medicine has been established next generation cancer therapy in treating diverse cancerous patients. Among the many approaches to comprehend precision medicine, the development of light activated nanotheranostic offerings a realistic personalized line of attack cancer treatment. The fast development of light-responsive functional HNCs promotes the research progression in new direction. Remotely triggering of HNCs by certain wavelength of light can effectively enhances cancer cells elimination, while preventing the normal tissues from the damage due to its non–invasive nature further supporting to reduce the side effect. Firstly, all these light therapies require the use of a pulsed laser light source to excite HNCs, in general, the very small focal area of the laser beam is not enough to guarantee the delivery of adequate photo

energy to sensitize NPs. Thus, much longer irradiation of laser light with accurate positional fine-tuning of the laser beam is require to ensure adequate photo energy supply to the entire solid tumor. The novel fiber optics technology currently being developed for micro endoscopic phototherapies, e.g. PDT/PTT, advancing the nanotheranostic approach in clinics with interstitial, endoscopic, intraoperative or laparoscopic light delivery into tumors[132]. Currently using surgical oncology tools tumors are removed surgically, but there may be many advantages to irradiate deeper and difficult-to-access tumors using light triggered nanotheranostics. The newly introduced wireless video capsule endoscopes with camera sensor, a light source, a battery and a wireless radiofrequency transmitter, can be considered alternative to conventional light delivery carriers for diagnosis and therapy of deep seated tumors[199]. Thus, tumors can be treated preoperatively.

Besides monotherapy, next generation nanotheranostics research is dedicated to design combined co therapy design instead of monotherapy. The recent pre-clinical investigations and clinical trials demonstrated that the therapeutic outcome of monotherapy is limited for the whole tumor elimination and averting cancer metastasis. The monotherapy is impartial for heterogeneous, diverse and complex tumors and just suitable for primary tumors. The synergy effect of PTT/PDT/chemo, is apparent for treating late stage cancer tumors and eliminating them preoperatively. In this regard, associations of the advantages of nanotechnology and TPE that hold great promise to selectively enhance PDT or PTT efficiency in deep seated solid tumors. As light triggered therapies are pioneered on the concept of phototoxicity, exploration of NIR light responsive HNCs and photochemistry is significant for future translation. We believe that, to achieve 100% tumor elimination without reoccurrence via PTT/PDT/chemo the a well-organized NIR light-responsive nanosystem is required. Owing to the interdisciplinary nature of this field, it is vital need of regular accelerations between scientists, academicians, engineers, clinicians, and industrial reformers. Exchanging the basic scientific ideas, clinical knowledge and discussions will advance the next generation cancer therapeutics and will bring the light triggered cancer nanotheranostics to the forefront of oncological diagnosis and intervention. The future of light responsive nanotheranostics lies in the development of a sole nano-therapeutic approach that encompasses its applicability in diagnosis as well as therapy.

In an attempt to improve diagnosis and treatment for patients with cancer diseases, few clinical firms have set up the light activated cancer treatments. ‘Theralase’ Toronto-based medical device manufacturer focuses on the discovery of small light-activated molecules and the development of laser systems and light activated drug that target and destroy cancer cells (https://theralase.com/photodynamic).The Germany based firm ‘Biofrontera AG’ has

advancing the treatment possibilities for non-melanoma skin cancer with the help of PDT (https://www.biofrontera.com/en/home-194.html). While on the other side 'CLINUVEL PHARMACEUTICALS' a multinational firm has made the remarkable progress in the palliative treatment of advanced stage cholangiocarcinoma, where a median time survival of 498 days has been reported in PDT as opposed to 98 days with conventional therapy (https://www.clinuvel.com/). The current short comings of light activated medical devices for cancer therapies are unfortunately undeniable, and therefore there is ongoing effort by scientific community and health industries to develop new technologies and improve our understanding of how these work in effort to develop not only more effective, but also more selective, therapies to reduce the burden on cancer patients.

V. Conclusion: The promise of physically stimulated cancer nanotheranostics

The potential clinical use of physically stimulated nanotheranostics in cancer treatment has not been thoroughly amplified. Numerous small animal preclinical reports are focused on the animal surface or superficial lesions experiments. A specialized probe for each nanotheranostics modality that would stimulate deep seated solid tumors would be ideal and promising but is technologically challenging in the short term. Present research directions are focused to design realistic theranostics probes that can adequately predict the diagnosis, therapy and therapy performance of a wide range of tumors, some of the light and magnetic probes are discussed in this review. Magnetic and photonic responsive nanotheranostics have enjoyed growing clinical adoption in many areas in particular cancer and will find increasing utilities in near future[200,201]. Inclusive strategies for designing novel nanostructures along with enhancing tumor image resolution in conjunction with conventional radiologic and molecular imaging specificity make nanotheranostics a next generation powerful modality. In the years to come, greater than before unification of biomedical engineers, scientists and clinicians will further enrich the physically stimulated nanotheranostics in patients. From a technological perspective, real time implementation of nanotheranostics to patients may not be far away. In addition to therapeutic approach, it is equally important to focus on intratumoral NPs loading and chemotherapeutic cargo release[202], both magnetic and light stimulation currently advancing the same.

We suggest extending the concept of physical stimulation beyond its current implication as individual therapeutic or diagnostic approach, to a comprehensive approach that uses multiple functionalities to aid or guide nanomedicine measures. As a result of huge inter-patient heterogeneity, personalized cancer nanotheranostics are desirable for achieving ideal

therapeutic efficacy without adverse side effects. In this regard, magnetic and light stimulation holds great potential as dual modality on single patient constitutes the whole trial, recently introduced as '*N*-of-1' clinical trial[203]. On the other side, instead of chemo-nanotheranostics alone, immune nanotheranostics in which tumor diagnostics and therapeutics are separately incorporated[204], is a genuine way of cancer diagnosis, patient stratification, and therapy response monitoring. With rapid advances in biomedical nanotechnologies and amplified recognition of magneto-plasmonic versatility in theranostics, many new implantable nanodevices based on magnetic-light-based functionalities are likely to emerge. It is projected that nanotheranostic will contribute a significant portion of the more than US$200-billion-per-year global medical device market[128] of personalised implanted medical devices, in next couple of years.

A few nanodevices and technologies that operate by the principles of physical stimulation discussed in this review are undergoing rigorous clinical trials at present. We need to observe the progress carefully whether these technologies fulfil their potential promise. New prospects are opening to nanotechnologists and clinicians, with the success or failure of these technologies, and will be revealing step for shaping future cancer theranostics. The review exchanged up to date information on technological development in cancer nanotheranostic to readers. Readers and scientist working in nanomedicine field can appreciate that all aspects of magnetic and light stimulation-from the choice of NPs to stimulation modality-must be thoroughly considered and tested before clinical translation. However, the clinical transformation of physically stimulated nanotheranostics has been delayed by several aspects, including NPs strange toxicity profiles, biodistribution, specificity of stimulation modality. Despite these and many other stumbling blocks, we envisage that physically stimulated cancer nanotheranostics accompanied with chemotherapeutic drugs and radio imaging modalities will be preferred as an effective therapeutics approach in the near future.

References:

[1] K.D. Miller, R.L. Siegel, C.C. Lin, A.B. Mariotto, J.L. Kramer, J.H. Rowland, K.D. Stein, R. Alteri, and A. Jemal, CA. Cancer J. Clin. **66**, 271 (2016).
[2] L. Zitvogel, L. Apetoh, F. Ghiringhelli, and G. Kroemer, Nat. Rev. Immunol. **8**, 59 (2008).
[3] L. Apetoh, F. Ghiringhelli, A. Tesniere, M. Obeid, C. Ortiz, A. Criollo, G. Mignot, M.C. Maiuri, E. Ullrich, P. Saulnier, H. Yang, S. Amigorena, B. Ryffel, F.J. Barrat, P. Saftig, F. Levi, R. Lidereau, C. Nogues, J.-P. Mira, A. Chompret, V. Joulin, F. Clavel-Chapelon, J. Bourhis, F. André, S. Delaloge, T. Tursz, G. Kroemer, and L. Zitvogel, Nat. Med. **13**, 1050 (2007).
[4] Q. Chen, H. Ke, Z. Dai, and Z. Liu, Biomaterials **73**, 214 (2015).
[5] A. Sneider, D. VanDyke, S. Paliwal, and P. Rai, Nanotheranostics **1**, 1 (2017).
[6] A. Sneider, D. VanDyke, S. Paliwal, and P. Rai, Nanotheranostics **1**, 1 (2017).
[7] R. Bardhan, S. Lal, A. Joshi, and N.J. Halas, Acc. Chem. Res. **44**, 936 (2011).
[8] S. Bhuniya, S. Maiti, E.-J. Kim, H. Lee, J.L. Sessler, K.S. Hong, and J.S. Kim, Angew. Chemie **126**, 4558 (2014).
[9] S.S. Kelkar and T.M. Reineke, Bioconjug. Chem. **22**, 1879 (2011).
[10] J. Nam, Y.S. Ha, S. Hwang, W. Lee, J. Song, J. Yoo, and S. Kim, Nanoscale **5**, 10175 (2013).
[11] A.J. Harnoy, I. Rosenbaum, E. Tirosh, Y. Ebenstein, R. Shaharabani, R. Beck, and R.J. Amir, J. Am. Chem. Soc. **136**, 7531 (2014).
[12] J. Hu, G. Zhang, and S. Liu, Chem. Soc. Rev. **41**, 5933 (2012).
[13] R. Liu, X. Zhao, T. Wu, and P. Feng, J. Am. Chem. Soc. **130**, 14418 (2008).
[14] R.H. Staff, M. Gallei, M. Mazurowski, M. Rehahn, R. Berger, K. Landfester, and D. Crespy, ACS Nano **6**, 9042 (2012).
[15] P. Kulkarni, M.K. Haldar, S. You, Y. Choi, and S. Mallik, Biomacromolecules **17**, 2507 (2016).
[16] P. Kulkarni, M.K. Haldar, P. Katti, C. Dawes, S. You, Y. Choi, and S. Mallik, Bioconjug. Chem. **27**, 1830 (2016).
[17] N.V. Rao, H. Ko, J. Lee, and J.H. Park, Front. Bioeng. Biotechnol. **6**, 110 (2018).
[18] J. Du, L.A. Lane, and S. Nie, J. Control. Release **219**, 205 (2015).
[19] H.S. El-Sawy, A.M. Al-Abd, T.A. Ahmed, K.M. El-Say, and V.P. Torchilin, ACS Nano **12**, 10636 (2018).
[20] S. Mura, J. Nicolas, and P. Couvreur, Nat. Mater. **12**, 991 (2013).
[21] M.A.C. Stuart, W.T.S. Huck, J. Genzer, M. Müller, C. Ober, M. Stamm, G.B. Sukhorukov, I. Szleifer, V. V. Tsukruk, M. Urban, F. Winnik, S. Zauscher, I. Luzinov, and S. Minko, Nat. Mater. **9**, 101 (2010).

[22] N.D. Thorat, H. Townely, G. Brennan, A.K. Parchur, C. Silien, J. Bauer, and S.A.M. Tofail, ACS Biomater. Sci. Eng. **5**, 2669 (2019).
[23] N.D. Thorat, G. Brennan, J. Bauer, C. Silien, and S.A.M. Tofail, in *Hybrid Nanostructures for Cancer Theranostics* (Elsevier, 2019), pp. 229–254.
[24] S.M. M., S. Veeranarayanan, T. Maekawa, and S.K. D., Adv. Drug Deliv. Rev. (2018).
[25] T. Maci, F. Le Pira, G. Quattrocchi, S. Di Nuovo, V. Perciavalle, and M. Zappia, Am. J. Alzheimer's Dis. Other Dementias® **27**, 107 (2012).
[26] S.T. Yeung, H. Martinez-Coria, R.R. Ager, C.J. Rodriguez-Ortiz, D. Baglietto-Vargas, and F.M. LaFerla, Brain Res. Bull. **117**, 10 (2015).
[27] Y. Brudno and D.J. Mooney, J. Control. Release **219**, 8 (2015).
[28] S. Lakshmanan, G.K. Gupta, P. Avci, R. Chandran, M. Sadasivam, A.E.S. Jorge, and M.R. Hamblin, Adv. Drug Deliv. Rev. **71**, 98 (2014).
[29] F. Wo, R. Xu, Y. Shao, Z. Zhang, M. Chu, D. Shi, and S. Liu, Theranostics **6**, 485 (2016).
[30] M. Wu and S. Huang, Mol. Clin. Oncol. **7**, 738 (2017).
[31] K. Kim and W.G. Lee, J. Mater. Chem. B **5**, 2726 (2017).
[32] L.A. Huber, T.A. Pereira, D.N. Ramos, L.C.D. Rezende, F.S. Emery, L.M. Sobral, A.M. Leopoldino, and R.F.V. Lopez, J. Biomed. Nanotechnol. **11**, 1975 (2015).
[33] G.-Y. Wan, Y. Liu, B.-W. Chen, Y.-Y. Liu, Y.-S. Wang, and N. Zhang, Cancer Biol. Med. **13**, 325 (2016).
[34] L. Rinaldi, V. Folliero, L. Palomba, C. Zannella, R. Isticato, R. Di Francia, M. Berretta, I. de Sio, L.E. Adinolfi, G. Morelli, S. Lastoria, L. Altucci, C. Pedone, M. Galdiero, and G. Franci, Oncotarget **9**, 32182 (2018).
[35] J. Baumgart, L. Humbert, É. Boulais, R. Lachaine, J.-J. Lebrun, and M. Meunier, Biomaterials **33**, 2345 (2012).
[36] N.D. Thorat, R.A. Bohara, M.R. Noor, D. Dhamecha, T. Soulimane, and S.A.M. Tofail, ACS Biomater. Sci. Eng. **3**, 1332 (2017).
[37] Y.I. Golovin, N.L. Klyachko, A.G. Majouga, M. Sokolsky, and A. V. Kabanov, J. Nanoparticle Res. **19**, 63 (2017).
[38] V.N. Binhi, *Magnetobiology : Underlying Physical Problems* (Academic Press, 2002).
[39] S. Lakshmanan, G.K. Gupta, P. Avci, R. Chandran, M. Sadasivam, A.E.S. Jorge, and M.R. Hamblin, Adv. Drug Deliv. Rev. **71**, 98 (2014).
[40] D. Mertz, O. Sandre, and S. Bégin-Colin, Biochim. Biophys. Acta - Gen. Subj. **1861**, 1617 (2017).
[41] B. Chertok, A.E. David, Y. Huang, and V.C. Yang, J. Control. Release **122**, 315 (2007).
[42] N. Maniotis, A. Makridis, E. Myrovali, A. Theopoulos, T. Samaras, and M. Angelakeris, J. Magn. Magn. Mater. **470**, 6 (2019).
[43] A.D. Grief and G. Richardson, J. Magn. Magn. Mater. **293**, 455 (2005).
[44] B. Sivaraman, G. Swaminathan, L. Moore, J. Fox, D. Seshadri, S. Dahal, I. Stoilov, M. Zborowski, R. Mecham, and A. Ramamurthi, Acta Biomater. **52**, 171 (2017).
[45] N. Depalo, R.M. Iacobazzi, G. Valente, I. Arduino, S. Villa, F. Canepa, V. Laquintana, E. Fanizza, M. Striccoli, A. Cutrignelli, A. Lopedota, L. Porcelli, A. Azzariti, M. Franco, M.L. Curri, and N. Denora, Nano Res. **10**, 2431 (2017).
[46] K. Ulbrich, K. Holá, V. Šubr, A. Bakandritsos, J. Tuček, and R. Zbořil, Chem. Rev. **116**, 5338 (2016).
[47] Y.-P. Wang, Y.-T. Liao, C.-H. Liu, J. Yu, H.R. Alamri, Z.A. Alothman, M.S.A. Hossain, Y. Yamauchi, and K.C.-W. Wu, ACS Biomater. Sci. Eng. **3**, 2366 (2017).
[48] C.N. Loynachan, G. Romero, M.G. Christiansen, R. Chen, R. Ellison, T.T. O'Malley, U.P. Froriep, D.M. Walsh, and P. Anikeeva, Adv. Healthc. Mater. **4**, 2100 (2015).
[49] S. Noh, S.H. Moon, T.-H. Shin, Y. Lim, and J. Cheon, Nano Today **13**, 61 (2017).
[50] A. Zakharchenko, N. Guz, A.M. Laradji, E. Katz, and S. Minko, Nat. Catal. **1**, 73 (2018).
[51] D. Mertz, O. Sandre, and S. Bégin-Colin, Biochim. Biophys. Acta - Gen. Subj. **1861**, 1617

(2017).
[52] A. Shademani, H. Zhang, J.K. Jackson, and M. Chiao, Adv. Funct. Mater. **27**, 1604558 (2017).
[53] O. Felfoul, M. Mohammadi, S. Taherkhani, D. de Lanauze, Y. Zhong Xu, D. Loghin, S. Essa, S. Jancik, D. Houle, M. Lafleur, L. Gaboury, M. Tabrizian, N. Kaou, M. Atkin, T. Vuong, G. Batist, N. Beauchemin, D. Radzioch, and S. Martel, Nat. Nanotechnol. **11**, 941 (2016).
[54] D. Shao, J. Li, X. Zheng, Y. Pan, Z. Wang, M. Zhang, Q.-X. Chen, W.-F. Dong, and L. Chen, Biomaterials **100**, 118 (2016).
[55] Y. Sheng, E. Beguin, H. Nesbitt, S. Kamila, J. Owen, L.C. Barnsley, B. Callan, C. O'Kane, N. Nomikou, R. Hamoudi, M.A. Taylor, M. Love, P. Kelly, D. O'Rourke, E. Stride, A.P. McHale, and J.F. Callan, J. Control. Release **262**, 192 (2017).
[56] C.-Y. Kuo, T.-Y. Liu, T.-Y. Chan, S.-C. Tsai, A. Hardiansyah, L.-Y. Huang, M.-C. Yang, R.-H. Lu, J.-K. Jiang, C.-Y. Yang, C.-H. Lin, and W.-Y. Chiu, Colloids Surfaces B Biointerfaces **140**, 567 (2016).
[57] A.K. Hauser, K.W. Anderson, and J.Z. Hilt, Nanomedicine **11**, 1769 (2016).
[58] N. Depalo, R.M. Iacobazzi, G. Valente, I. Arduino, S. Villa, F. Canepa, V. Laquintana, E. Fanizza, M. Striccoli, A. Cutrignelli, A. Lopedota, L. Porcelli, A. Azzariti, M. Franco, M.L. Curri, and N. Denora, Nano Res. **10**, 2431 (2017).
[59] A. Al Faraj, A.P. Shaik, and A.S. Shaik, Int. J. Nanomedicine **10**, 157 (2015).
[60] R. Grifantini, M. Taranta, L. Gherardini, I. Naldi, M. Parri, A. Grandi, A. Giannetti, S. Tombelli, G. Lucarini, L. Ricotti, S. Campagnoli, E. De Camilli, G. Pelosi, F. Baldini, A. Menciassi, G. Viale, P. Pileri, and C. Cinti, J. Control. Release **280**, 76 (2018).
[61] F. Munoz, G. Alici, and W. Li, J. Med. Device. **10**, 011004 (2015).
[62] N.D. Thorat, R.A. Bohara, V. Malgras, S.A.M. Tofail, T. Ahamad, S.M. Alshehri, K.C.-W. Wu, and Y. Yamauchi, ACS Appl. Mater. Interfaces acsami.6b02616 (2016).
[63] N.D. Thorat, O.M. Lemine, R.A. Bohara, K. Omri, L. El Mir, and S.A.M. Tofail, Phys. Chem. Chem. Phys. **33**, 941 (2016).
[64] A.K. Hauser, R.J. Wydra, N.A. Stocke, K.W. Anderson, and J.Z. Hilt, J. Control. Release **219**, 76 (2015).
[65] Z. Hedayatnasab, F. Abnisa, and W.M.A.W. Daud, Mater. Des. **123**, 174 (2017).
[66] D. Chang, M. Lim, J.A.C.M. Goos, R. Qiao, Y.Y. Ng, F.M. Mansfeld, M. Jackson, T.P. Davis, and M. Kavallaris, Front. Pharmacol. **9**, 831 (2018).
[67] S. Laurent, S. Dutz, U.O. Häfeli, and M. Mahmoudi, Adv. Colloid Interface Sci. **166**, 8 (2011).
[68] E.A. Périgo, G. Hemery, O. Sandre, D. Ortega, E. Garaio, F. Plazaola, and F.J. Teran, J. Appl. Phys. **2**, 83921 (2015).
[69] N.D. Thorat, G. Brennan, J. Bauer, C. Silien, and S.A.M. Tofail, *Strengths and Limitations of Translating the Hybrid Nanostructures to the Clinic* (Elsevier, 2019).
[70] N.D. Thorat, R. Bohara, H.M. Yadav, S.V. Otari, S.H. Pawar, and S.A.M. Tofail, Nanoarchitectonics Smart Deliv. Drug Target. 589 (2016).
[71] N.D. Thorat, V.M. Khot, A.B. Salunkhe, A.I. Prasad, R.S. Ningthoujam, and S.H. Pawar, J. Phys. D. Appl. Phys. **46**, 105003 (2013).
[72] P. Dhar and L. Sirisha Maganti, J. Appl. Phys. **122**, 054902 (2017).
[73] L.M. Bauer, S.F. Situ, M.A. Griswold, and A.C.S. Samia, Nanoscale **8**, 12162 (2016).
[74] E.C. Abenojar, S. Wickramasinghe, J. Bas-Concepcion, and A.C.S. Samia, Prog. Nat. Sci. Mater. Int. **26**, 440 (2016).
[75] A. Jordan, P. Wust, H. Fähling, W. John, A. Hinz, and R. Felix, Int. J. Hyperth. **9**, 51 (1993).
[76] K. El-Boubbou, Nanomedicine **13**, 953 (2018).
[77] D. Chang, M. Lim, J.A.C.M. Goos, R. Qiao, Y.Y. Ng, F.M. Mansfeld, M. Jackson, T.P. Davis, and M. Kavallaris, Front. Pharmacol. **9**, 831 (2018).

[78] N.R. Datta, S. Krishnan, D.E. Speiser, E. Neufeld, N. Kuster, S. Bodis, and H. Hofmann, Cancer Treat. Rev. **50**, 217 (2016).
[79] T.R. Oliveira, P.R. Stauffer, C.-T. Lee, C.D. Landon, W. Etienne, K.A. Ashcraft, K.L. McNerny, A. Mashal, J. Nouls, P.F. Maccarini, W.F. Beyer, B. Inman, and M.W. Dewhirst, Int. J. Hyperth. **29**, 835 (2013).
[80] B.T. Mai, P.B. Balakrishnan, M.J. Barthel, F. Piccardi, D. Niculaes, F. Marinaro, S. Fernandes, A. Curcio, H. Kakwere, G. Autret, R. Cingolani, F. Gazeau, and T. Pellegrino, ACS Appl. Mater. Interfaces **11**, 5727 (2019).
[81] E. Alphandéry, A. Idbaih, C. Adam, J.-Y. Delattre, C. Schmitt, F. Guyot, and I. Chebbi, Biomaterials **141**, 210 (2017).
[82] N.A. Stocke, P. Sethi, A. Jyoti, R. Chan, S.M. Arnold, J.Z. Hilt, and M. Upreti, Biomaterials **120**, 115 (2017).
[83] X. Yao, X. Niu, K. Ma, P. Huang, J. Grothe, S. Kaskel, and Y. Zhu, Small **13**, 1602225 (2017).
[84] E. Guisasola, L. Asín, L. Beola, J.M. de la Fuente, A. Baeza, and M. Vallet-Regí, ACS Appl. Mater. Interfaces **10**, 12518 (2018).
[85] K. Mahmoudi, A. Bouras, D. Bozec, R. Ivkov, and C. Hadjipanayis, Int. J. Hyperth. **34**, 1316 (2018).
[86] Y. Cheng, M.E. Muroski, D.C.M.C. Petit, R. Mansell, T. Vemulkar, R.A. Morshed, Y. Han, I. V. Balyasnikova, C.M. Horbinski, X. Huang, L. Zhang, R.P. Cowburn, and M.S. Lesniak, J. Control. Release **223**, 75 (2016).
[87] J. Alonso, H. Khurshid, J. Devkota, Z. Nemati, N.K. Khadka, H. Srikanth, J. Pan, and M.-H. Phan, J. Appl. Phys. **119**, 083904 (2016).
[88] M. Gonzales and K.M. Krishnan, J. Magn. Magn. Mater. **293**, 265 (2005).
[89] R. V Ferreira, T.M. da M. Martins, A.M. Goes, J.D. Fabris, L.C.D. Cavalcante, L.E.F. Outon, and R.Z. Domingues, Nanotechnology **27**, 085105 (2016).
[90] M. Moros, J. Idiago-López, L. Asín, E. Moreno-Antolín, L. Beola, V. Grazú, R.M. Fratila, L. Gutiérrez, and J.M. de la Fuente, Adv. Drug Deliv. Rev. (2018).
[91] Y. Guo, Y. Zhang, J. Ma, Q. Li, Y. Li, X. Zhou, D. Zhao, H. Song, Q. Chen, and X. Zhu, J. Control. Release **272**, 145 (2018).
[92] M. Li, W. Bu, J. Ren, J. Li, L. Deng, M. Gao, X. Gao, and P. Wang, Theranostics **8**, 693 (2018).
[93] I. Sato, M. Umemura, K. Mitsudo, H. Fukumura, J.-H. Kim, Y. Hoshino, H. Nakashima, M. Kioi, R. Nakakaji, M. Sato, T. Fujita, U. Yokoyama, S. Okumura, H. Oshiro, H. Eguchi, I. Tohnai, and Y. Ishikawa, Sci. Rep. **6**, 24629 (2016).
[94] S. V Spirou, M. Basini, A. Lascialfari, C. Sangregorio, and C. Innocenti, Nanomater. (Basel, Switzerland) **8**, (2018).
[95] N.R. Datta, S.G. Ordóñez, U.S. Gaipl, M.M. Paulides, H. Crezee, J. Gellermann, D. Marder, E. Puric, and S. Bodis, Cancer Treat. Rev. **41**, 742 (2015).
[96] S. Spirou, S. Costa Lima, P. Bouziotis, S. Vranješ-Djurić, E. Efthimiadou, A. Laurenzana, A. Barbosa, I. Garcia-Alonso, C. Jones, D. Jankovic, O. Gobbo, S. V. Spirou, S.A. Costa Lima, P. Bouziotis, S. Vranješ-Djurić, E.K. Efthimiadou, A. Laurenzana, A.I. Barbosa, I. Garcia-Alonso, C. Jones, D. Jankovic, and O.L. Gobbo, Nanomaterials **8**, 306 (2018).
[97] R. Ivkov, Int. J. Hyperth. **29**, 703 (2013).
[98] S. Dutz, R. Hergt, J. Mürbe, R. Müller, M. Zeisberger, W. Andrä, J. Töpfer, and M.E. Bellemann, J. Magn. Magn. Mater. **308**, 305 (2007).
[99] N.D. Thorat, K.P. Shinde, S.H. Pawar, K.C. Barick, C.A. Betty, and R.S. Ningthoujam, Dalt. Trans. **41**, 3060 (2012).
[100] Z. Zhou, R. Bai, J. Munasinghe, Z. Shen, L. Nie, and X. Chen, ACS Nano **11**, 5227 (2017).
[101] T.-H. Shin, J. Choi, S. Yun, I.-S. Kim, H.-T. Song, Y. Kim, K.I. Park, and J. Cheon, ACS

Nano **8**, 3393 (2014).
[102] E. Polo, P. del Pino, A. Pardo, P. Taboada, and B. Pelaz, in *Nanooncology* (Springer, Cham, 2018), pp. 239–279.
[103] Y. Javed, K. Akhtar, H. Anwar, and Y. Jamil, J. Nanoparticle Res. **19**, 366 (2017).
[104] M.K. Yu, J. Park, and S. Jon, Drug Deliv. Transl. Res. **2**, 3 (2012).
[105] N.D. Thorat, R.A. Bohara, H.M. Yadav, and S.A.M. Tofail, RSC Adv. **6**, 94967 (2016).
[106] N.D. Thorat, R.A. Bohara, S.A.M. Tofail, Z.A. Alothman, M.J.A. Shiddiky, M.S. A Hossain, Y. Yamauchi, and K.C.-W. Wu, Eur. J. Inorg. Chem. **2016**, 4586 (2016).
[107] T.-H. Shin, Y. Choi, S. Kim, and J. Cheon, Chem. Soc. Rev. **44**, 4501 (2015).
[108] L.M. Bauer, S.F. Situ, M.A. Griswold, and A.C.S. Samia, J. Phys. Chem. Lett. **6**, 2509 (2015).
[109] Z.W. Tay, P. Chandrasekharan, A. Chiu-Lam, D.W. Hensley, R. Dhavalikar, X.Y. Zhou, E.Y. Yu, P.W. Goodwill, B. Zheng, C. Rinaldi, and S.M. Conolly, ACS Nano **12**, 3699 (2018).
[110] B. Gleich and J. Weizenecker, Nature **435**, 1214 (2005).
[111] M.H. Pablico-Lansigan, S.F. Situ, and A.C.S. Samia, Nanoscale **5**, 4040 (2013).
[112] T. Knopp, N. Gdaniec, and M. Möddel, Phys. Med. Biol. **62**, R124 (2017).
[113] K.R. Minard, in *Encycl. Spectrosc. Spectrom.* (Springer International Publishing, Cham, 2016), pp. 685–692.
[114] Y. Hu, S. Mignani, J.-P. Majoral, M. Shen, and X. Shi, Chem. Soc. Rev. **47**, 1874 (2018).
[115] T.-H. Shin, Y. Choi, S. Kim, and J. Cheon, Chem. Soc. Rev. **44**, 4501 (2015).
[116] M. Mahmoudi, H. Hosseinkhani, M. Hosseinkhani, S. Boutry, A. Simchi, W.S. Journeay, K. Subramani, and S. Laurent, Chem. Rev. **111**, 253 (2011).
[117] D.-H. Kim, J. Chen, R.A. Omary, and A.C. Larson, Theranostics **5**, 477 (2015).
[118] J. Lu, J. Sun, F. Li, J. Wang, J. Liu, D. Kim, C. Fan, T. Hyeon, and D. Ling, J. Am. Chem. Soc. **140**, 10071 (2018).
[119] J. Choi, S. Kim, D. Yoo, T.-H. Shin, H. Kim, M.D. Gomes, S.H. Kim, A. Pines, and J. Cheon, Nat. Mater. **16**, 537 (2017).
[120] J. Lee, A.C. Gordon, H. Kim, W. Park, S. Cho, B. Lee, A.C. Larson, E.A. Rozhkova, and D.-H. Kim, Biomaterials **109**, 69 (2016).
[121] J. Lin, P. Xin, L. An, Y. Xu, C. Tao, Q. Tian, Z. Zhou, B. Hu, and S. Yang, Chem. Commun. **55**, 478 (2019).
[122] A. Tomitaka, H. Arami, A. Raymond, A. Yndart, A. Kaushik, R.D. Jayant, Y. Takemura, Y. Cai, M. Toborek, and M. Nair, Nanoscale **9**, 764 (2017).
[123] S. Cho, W. Park, and D.-H. Kim, ACS Appl. Mater. Interfaces **9**, 101 (2017).
[124] W. Park, A.C. Gordon, S. Cho, X. Huang, K.R. Harris, A.C. Larson, and D.-H. Kim, ACS Appl. Mater. Interfaces **9**, 13819 (2017).
[125] D. Hensley, Z.W. Tay, R. Dhavalikar, B. Zheng, P. Goodwill, C. Rinaldi, and S. Conolly, Phys. Med. Biol. **62**, 3483 (2017).
[126] J.W.M. Bulte, Adv. Drug Deliv. Rev. (2018).
[127] E.E. Mason, C.Z. Cooley, S.F. Cauley, M.A. Griswold, S.M. Conolly, and L.L. Wald, Int. J. Magn. Part. Imaging **3**, (2017).
[128] S.H. Yun and S.J.J. Kwok, Nat. Biomed. Eng. **1**, 0008 (2017).
[129] P. Zhang, C. Hu, W. Ran, J. Meng, Q. Yin, and Y. Li, Theranostics **6**, 948 (2016).
[130] S. Gai, G. Yang, P. Yang, F. He, J. Lin, D. Jin, and B. Xing, Nano Today **19**, 146 (2018).
[131] D. de Melo-Diogo, C. Pais-Silva, D.R. Dias, A.F. Moreira, and I.J. Correia, Adv. Healthc. Mater. **6**, 1700073 (2017).
[132] A.L. Chin, Y. Zhong, and R. Tong, Biomater. Sci. **5**, 1491 (2017).
[133] S.S. Lucky, K.C. Soo, and Y. Zhang, Chem. Rev. **115**, 1990 (2015).
[134] T.C. Zhu and J.C. Finlay, Med. Phys. **35**, 3127 (2008).
[135] Y. Cheng, H. Cheng, C. Jiang, X. Qiu, K. Wang, W. Huan, A. Yuan, J. Wu, and Y. Hu,

Nat. Commun. **6**, 8785 (2015).
[136] A. Bansal, F. Yang, T. Xi, Y. Zhang, and J.S. Ho, Proc. Natl. Acad. Sci. **115**, 1469 (2018).
[137] Y. Cheng, H. Cheng, C. Jiang, X. Qiu, K. Wang, W. Huan, A. Yuan, J. Wu, and Y. Hu, Nat. Commun. **6**, 8785 (2015).
[138] Y. Zhang, F. Wang, C. Liu, Z. Wang, L. Kang, Y. Huang, K. Dong, J. Ren, and X. Qu, ACS Nano **12**, 651 (2018).
[139] C. Yao, W. Wang, P. Wang, M. Zhao, X. Li, and F. Zhang, Adv. Mater. **30**, 1704833 (2018).
[140] D. Cui, J. Huang, X. Zhen, J. Li, Y. Jiang, and K. Pu, Angew. Chemie Int. Ed. (2019).
[141] S. Xu, X. Zhu, C. Zhang, W. Huang, Y. Zhou, and D. Yan, Nat. Commun. **9**, 2053 (2018).
[142] T. Lin, X. Zhao, S. Zhao, H. Yu, W. Cao, W. Chen, H. Wei, and H. Guo, Theranostics **8**, 990 (2018).
[143] K. Zhang, Y. Zhang, X. Meng, H. Lu, H. Chang, H. Dong, and X. Zhang, Biomaterials **185**, 301 (2018).
[144] Q. Jia, J. Ge, W. Liu, X. Zheng, S. Chen, Y. Wen, H. Zhang, and P. Wang, Adv. Mater. **30**, 1706090 (2018).
[145] Z. Wang, Y. Zhang, E. Ju, Z. Liu, F. Cao, Z. Chen, J. Ren, and X. Qu, Nat. Commun. **9**, 3334 (2018).
[146] J. Liu, P. Du, H. Mao, L. Zhang, H. Ju, and J. Lei, Biomaterials **172**, 83 (2018).
[147] Z. Dong, L. Feng, Y. Hao, M. Chen, M. Gao, Y. Chao, H. Zhao, W. Zhu, J. Liu, C. Liang, Q. Zhang, and Z. Liu, J. Am. Chem. Soc. **140**, 2165 (2018).
[148] B. Mao, C. Liu, W. Zheng, X. Li, R. Ge, H. Shen, X. Guo, Q. Lian, X. Shen, and C. Li, Biomaterials **161**, 306 (2018).
[149] X. Zhang, X. Chen, H.-Y. Wang, H.-R. Jia, and F.-G. Wu, Adv. Ther. 1800140 (2019).
[150] Z. Yu, P. Zhou, W. Pan, N. Li, and B. Tang, Nat. Commun. **9**, 5044 (2018).
[151] M.G. Mokwena, C.A. Kruger, M.-T. Ivan, and A. Heidi, Photodiagnosis Photodyn. Ther. **22**, 147 (2018).
[152] X. Li, N. Kwon, T. Guo, Z. Liu, and J. Yoon, Angew. Chemie Int. Ed. **57**, 11522 (2018).
[153] A. Bansal, F. Yang, T. Xi, Y. Zhang, and J.S. Ho, Proc. Natl. Acad. Sci. U. S. A. **115**, 1469 (2018).
[154] K. Yamagishi, I. Kirino, I. Takahashi, H. Amano, S. Takeoka, Y. Morimoto, and T. Fujie, Nat. Biomed. Eng. **3**, 27 (2019).
[155] Y. Lee and D.-H. Kim, Nat. Biomed. Eng. **3**, 5 (2019).
[156] L. Hu, P. Wang, M. Zhao, L. Liu, L. Zhou, B. Li, F.H. Albaqami, A.M. El-Toni, X. Li, Y. Xie, X. Sun, and F. Zhang, Biomaterials **163**, 154 (2018).
[157] J. Kim, W. Park, D. Kim, E.S. Lee, D.H. Lee, S. Jeong, J.M. Park, and K. Na, Adv. Funct. Mater. 1900084 (2019).
[158] E.D. Onal and K. Guven, J. Phys. Chem. C **121**, 684 (2017).
[159] Y. Liu, P. Bhattarai, Z. Dai, and X. Chen, Chem. Soc. Rev. **48**, 2053 (2019).
[160] R.S. Riley and E.S. Day, Wiley Interdiscip. Rev. Nanomedicine Nanobiotechnology **9**, e1449 (2017).
[161] D. de Melo-Diogo, C. Pais-Silva, D.R. Dias, A.F. Moreira, and I.J. Correia, Adv. Healthc. Mater. **6**, 1700073 (2017).
[162] J. Oh, H.-J. Yoon, and J.-H. Park, J. Mater. Chem. B **2**, 2592 (2014).
[163] F. Chen and W. Cai, Nanomedicine **10**, 1 (2015).
[164] Y. Yang, J. Aw, and B. Xing, Nanoscale **9**, 3698 (2017).
[165] Y. Liu, Z. Yang, X. Huang, G. Yu, S. Wang, Z. Zhou, Z. Shen, W. Fan, Y. Liu, M. Davisson, H. Kalish, G. Niu, Z. Nie, and X. Chen, ACS Nano **12**, 8129 (2018).
[166] C. Lee, H.S. Hwang, S. Lee, B. Kim, J.O. Kim, K.T. Oh, E.S. Lee, H.-G. Choi, and Y.S. Youn, Adv. Mater. **29**, 1605563 (2017).
[167] T. Sugiura, D. Matsuki, J. Okajima, A. Komiya, S. Mori, S. Maruyama, and T. Kodama,

Nano Res. **8**, 3842 (2015).
[168] M. Singh, E. Nabavi, Y. Zhou, M.E. Gallina, H. Zhao, P. Ruenraroengsak, A.E. Porter, D. Ma, A.E.G. Cass, G.B. Hanna, and D.S. Elson, Nanotheranostics **3**, 89 (2019).
[169] M.S. Beg, F. Adhami, L. Xuan, J. Hodges, J. Meyer, E. Halm, and S. Pruitt, J. Clin. Oncol. **32**, 577 (2017).
[170] A.K. Parchur, G. Sharma, J.M. Jagtap, V.R. Gogineni, P.S. LaViolette, M.J. Flister, S.B. White, and A. Joshi, ACS Nano **12**, 6597 (2018).
[171] Y. Li, G. Liu, J. Ma, J. Lin, H. Lin, G. Su, D. Chen, S. Ye, X. Chen, X. Zhu, and Z. Hou, J. Control. Release **258**, 95 (2017).
[172] H. Hu, C. Xiao, H. Wu, Y. Li, Q. Zhou, Y. Tang, C. Yu, X. Yang, and Z. Li, ACS Appl. Mater. Interfaces **9**, 42225 (2017).
[173] L. Song, Z. Pan, H. Zhang, Y. Li, Y. Zhang, J. Lin, G. Su, S. Ye, L. Xie, Y. Li, and Z. Hou, J. Mater. Chem. B **5**, 6835 (2017).
[174] H. Zhu, P. Cheng, P. Chen, and K. Pu, Biomater. Sci. **6**, 746 (2018).
[175] H. Yan, W. Shang, X. Sun, L. Zhao, X. Wang, S. Zhang, N. Xu, W. Xu, J. Tian, and F. Kang, Nanoscale **11**, 706 (2019).
[176](2008).
[177] F.O. Obiweluozor, G.A. Emechebe, A.P. Tiwari, J.Y. Kim, C.H. Park, and C.S. Kim, Int. J. Nanomedicine **13**, 6375 (2018).
[178] H. Lee, Y. Lee, C. Song, H.R. Cho, R. Ghaffari, T.K. Choi, K.H. Kim, Y.B. Lee, D. Ling, H. Lee, S.J. Yu, S.H. Choi, T. Hyeon, and D.-H. Kim, Nat. Commun. **6**, 10059 (2015).
[179] J. Kress, D.J. Rohrbach, K.A. Carter, D. Luo, C. Poon, S. Aygun-Sunar, S. Shao, S. Lele, J.F. Lovell, and U. Sunar, Sci. Rep. **7**, 15578 (2017).
[180] S. Protti, A. Albini, R. Viswanathan, and A. Greer, Photochem. Photobiol. **93**, 1139 (2017).
[181] H.-W. Liu, Y. Liu, P. Wang, and X.-B. Zhang, Methods Appl. Fluoresc. **5**, 012003 (2017).
[182] Y. Shen, A.J. Shuhendler, D. Ye, J.-J. Xu, and H.-Y. Chen, Chem. Soc. Rev. **45**, 6725 (2016).
[183] M. Lan, S. Zhao, Z. Zhang, L. Yan, L. Guo, G. Niu, J. Zhang, J. Zhao, H. Zhang, P. Wang, G. Zhu, C.-S. Lee, and W. Zhang, Nano Res. **10**, 3113 (2017).
[184] D. Gao, R.R. Agayan, H. Xu, M.A. Philbert, and R. Kopelman, Nano Lett. **6**, 2383 (2006).
[185] N.J. Durr, T. Larson, D.K. Smith, B.A. Korgel, K. Sokolov, and A. Ben-Yakar, Nano Lett. **7**, 941 (2007).
[186] L. Gao, J. Fei, J. Zhao, H. Li, Y. Cui, and J. Li, ACS Nano **6**, 8030 (2012).
[187] H. Wang, Y. Sun, J. Yi, J. Fu, J. Di, A. del Carmen Alonso, and S. Zhou, Biomaterials **53**, 117 (2015).
[188] M. Lan, L. Guo, S. Zhao, Z. Zhang, Q. Jia, L. Yan, J. Xia, H. Zhang, P. Wang, and W. Zhang, Adv. Ther. **1**, 1800077 (2018).
[189] B. Geng, D. Yang, D. Pan, L. Wang, F. Zheng, W. Shen, C. Zhang, and X. Li, Carbon N. Y. **134**, 153 (2018).
[190] S.M. Ardekani, A. Dehghani, M. Hassan, M. Kianinia, I. Aharonovich, and V.G. Gomes, Chem. Eng. J. **330**, 651 (2017).
[191] Y. Li, G. Bai, S. Zeng, and J. Hao, ACS Appl. Mater. Interfaces **11**, 4737 (2019).
[192] R.-Q. Li, C. Zhang, B.-R. Xie, W.-Y. Yu, W.-X. Qiu, H. Cheng, and X.-Z. Zhang, Biomaterials **194**, 84 (2019).
[193] B. Sun, L. Wang, Q. Li, P. He, H. Liu, H. Wang, Y. Yang, and J. Li, Biomacromolecules **18**, 3506 (2017).
[194] A. Sourdon, M. Gary-Bobo, M. Maynadier, M. Garcia, J. Majoral, A. Caminade, O. Mongin, and M. Blanchard-Desce, Chem. – A Eur. J. **25**, 3637 (2019).
[195] J. Xu, P. Yang, M. Sun, H. Bi, B. Liu, D. Yang, S. Gai, F. He, and J. Lin, ACS Nano **11**, 4133 (2017).

[196] J.G. Croissant, J.I. Zink, L. Raehm, and J.-O. Durand, Adv. Healthc. Mater. **7**, 1701248 (2018).
[197] S. Wang, J. Liu, G. Feng, L.G. Ng, and B. Liu, Adv. Funct. Mater. **29**, 1808365 (2019).
[198] N. Alifu, L. Yan, H. Zhang, A. Zebibula, Z. Zhu, W. Xi, A.W. Roe, B. Xu, W. Tian, and J. Qian, Dye. Pigment. **143**, 76 (2017).
[199] E. Redondo-Cerezo, A.D. Sánchez-Capilla, P. De La Torre-Rubio, and J. De Teresa, World J. Gastroenterol. **20**, 15664 (2014).
[200] S.V. Otari, M. Kumar, M.Z. Anwar, N.D. Thorat, S.K.S. Patel, D. Lee, J.H. Lee, J.-K. Lee, Y.C. Kang, and L. Zhang, Sci. Rep. **7**, (2017).
[201] R.M. Patil, N.D. Thorat, P.B. Shete, S.V. Otari, B.M. Tiwale, and S.H. Pawar, Mater. Sci. Eng. C **59**, 702 (2016).
[202] S. Kunjachan, J. Ehling, G. Storm, F. Kiessling, and T. Lammers, Chem. Rev. **115**, 10907 (2015).
[203] N.J. Schork, Nature **520**, 609 (2015).
[204] H. Chen, W. Zhang, G. Zhu, J. Xie, and X. Chen, Nat. Rev. Mater. **2**, 17024 (2017).